2012

Glutaredoxin 1 Protects Dopaminergic Cells by Increased Protein Glutathionylation in Experimental Parkinson's Disease

Humberto Rodriguez-Rocha
University of Nebraska-Lincoln

Aracely Garcia Garcia
University of Nebraska-Lincoln

Laura Zavala-Flores
University of Nebraska-Lincoln

Sumin Li
University of Nebraska - Lincoln

Nandakumar Madayiputhiya
University of Nebraska - Lincoln, nmadayiputhiya2@unl.edu

See next page for additional authors

Antioxidants & Redox Signaling

Antioxid Redox Signal. 17(12): 1676-1693
https://www.ncbi.nlm.nih.gov/pmc/articles/PMC3474191/

Glutaredoxin 1 Protects Dopaminergic Cells by Increased Protein Glutathionylation in Experimental Parkinson's Disease

Humberto Rodriguez-Rocha[12*], Aracely Garcia Garcia[12*], Laura Zavala-Flores[12], Sumin Li[12], Nandakumar Madayiputhiya[13], Rodrigo Franco[12]

[1]. *Redox Biology Center, University of Nebraska-Lincoln, Lincoln, Nebraska.*

[2]. *School of Veterinary Medicine and Biomedical Sciences, University of Nebraska-Lincoln, Lincoln, Nebraska.*

[3]. *Department of Biochemistry, University of Nebraska-Lincoln, Lincoln, Nebraska.*

Address correspondence to: *Dr. Rodrigo Franco, Redox Biology Center and School of Veterinary Medicine and Biomedical Sciences, 114 VBS E. Campus Loop and Fair Street, University of Nebraska-Lincoln, Lincoln, NE 68583. E-mail:*rfrancocruz2@unl.edu

*. Both authors contributed equally to this work.

DOI: 10.1089/ars.2011.4474
Published in print: 15 December 2012

Abstract

Aims: Chronic exposure to environmental toxicants, such as paraquat, has been suggested as a risk factor for Parkinson's disease (PD). Although dopaminergic cell death in PD is associated with oxidative damage, the molecular mechanisms involved remain elusive. Glutaredoxins (GRXs) utilize the

reducing power of glutathione to modulate redox-dependent signaling pathways by protein glutathionylation. We aimed to determine the role of GRX1 and protein glutathionylation in dopaminergic cell death. ***Results:*** In dopaminergic cells, toxicity induced by paraquat or 6-hydroxydopamine (6-OHDA) was inhibited by GRX1 overexpression, while its knock-down sensitized cells to paraquat-induced cell death. Dopaminergic cell death was paralleled by protein deglutathionylation, and this was reversed by GRX1. Mass spectrometry analysis of immunoprecipitated glutathionylated proteins identified the actin binding flightless-1 homolog protein (FLI-I) and the RalBP1-associated Eps domain-containing protein 2 (REPS2/POB1) as targets of glutathionylation in dopaminergic cells. Paraquat induced the degradation of FLI-I and REPS2 proteins, which corresponded with the activation of caspase 3 and cell death progression. GRX1 overexpression reduced both the degradation and deglutathionylation of FLI-I and REPS2, while stable overexpression of REPS2 reduced paraquat toxicity. A decrease in glutathionylated proteins and REPS2 levels was also observed in the substantia nigra of mice treated with paraquat. ***Innovation:*** We have identified novel protein targets of glutathionylation in dopaminergic cells and demonstrated the protective role of GRX1-mediated protein glutathionylation against paraquat-induced toxicity. ***Conclusions:*** These results demonstrate a protective role for GRX1 and increased protein glutathionylation in dopaminergic cell death induced by paraquat, and identify a novel protective role for REPS2. *Antioxid. Redox Signal.* 17, 1676–1693.

Introduction

PARKINSON'S DISEASE (PD) is characterized by the selective loss of dopaminergic neurons of the substantia nigra pars compacta (SNpc) (71). Previous studies have indicated that exposure to environmental toxins such

as herbicides and pesticides increase the risk of developing PD by increasing oxidative stress and mitochondrial dysfunction (24, 25, 28, 80). Although dopaminergic cell death is a cardinal feature of PD, the mechanisms and pathways involved remain unclear. Current evidence supports a role for mitochondrial dysfunction, oxidative stress, and abnormal protein accumulation as early triggers of neuronal death in PD (50, 62, 92). Oxidative damage to lipids, proteins, and DNA, as well as a decrease in the levels of the low molecular thiol antioxidant glutathione (GSH), have been detected in samples from individuals with PD (1, 2, 22, 42, 60). Oxidative stress in PD is linked primarily with mitochondrial dysfunction as demonstrated by reports showing decreased activity of the mitochondrial electron transport chain in the substantia nigra of patients with PD (35, 70, 73).

An increase in protein oxidation has been reported in brains from PD patients as evidenced by the accumulation of oxidative and nitrosative protein modifications (1, 21). An important cellular target or sensor of reactive species is the thiol group (SH) of the amino acid cysteine. Redox-sensitive cysteines in proteins undergo oxidative modifications in response to reactive oxygen (ROS) or nitrogen species, thereby modulating protein function, activity, and/or localization. Oxidation and reduction of cellular thiols are thought to be major mechanisms by which oxidative stress is integrated into cellular signal transduction pathways (61, 88). Protein glutathionylation is defined as the reversible formation of a mixed-disulfide between GSH and protein thiols involved in the redox-regulation of protein function (19, 55). Previous studies have demonstrated the occurrence of protein glutathionylation/deglutathionylation in dopaminergic cells. Mitochondrial protein deglutathionylation has been reported in response to oxidative stress in dopaminergic cells (56). In contrast, increased

glutathionylation of the mitochondrial NADP(+)-dependent isocitrate dehydrogenase (IDPm) was reported in the MPTP mouse PD model (47). However, the role of protein glutathionylation in dopaminergic cell death in other experimental PD models, particularly those associated with environmental toxicants, has not been studied in detail.

Innovation

Dopaminergic cell death in PD is associated with increased oxidative damage. However, the mechanisms by which redox signaling regulates cell death progression are still unclear. We demonstrated, for the first time, the protective role of the thiol oxidoreductase GRX1 against dopaminergic cell death induced by the environmental pesticide paraquat, and the dopaminergic toxin 6-OHDA. We also demonstrated that the protective effect of GRX1 is ascribed to the regulation of glutathionylation/deglutathionylation of cellular protein targets. Additionally, we identified novel molecular targets for protein glutathionylation that include the actin-binding protein FLI-I and the RalBP1-associated Eps domain-containing protein REPS2/POB1; and for the case of REPS2, we demonstrated its protective effect against dopaminergic cell death induced by paraquat. Finally, we found that overall PSSG and REPS2 levels were decreased in the substantia nigra of mice treated with paraquat.

In this study, we demonstrated a protective role of GRX1 and protein glutathionylation in dopaminergic cell death induced by paraquat and 6-OHDA. More importantly, we identified the actin binding flightless-1 homolog protein (FLI-I) and the RalBP1-associated Eps domain-containing

protein 2 (REPS2/POB1) as novel targets of protein glutathionylation in dopaminergic cells. Paraquat-induced dopaminergic cell death was paralleled by degradation of FLI-I and REPS2 protein, and overexpression of REPS2 significantly reduced dopaminergic cell death induced by paraquat. A decrease in glutathionylated residues and REPS2 protein levels was also observed in the substantia nigra of mice treated with paraquat. These results describe a protective role for GRX1-mediated protein glutathionylation in dopaminergic cell death associated with PD and demonstrate a novel protective role for REPS2.

Results

GRX1 protects against experimental PD

Recent studies have demonstrated that the exposure to environmental toxins, such as paraquat, is strongly associated to an elevated risk of developing PD progression (5, 14, 80), which might be mediated by increased oxidative stress and mitochondria dysfunction (24, 27, 74). The oxidoreductase GRX1 has been shown to exert a protective effect against dopamine and MPTP toxicity in neuronal cells (16, 17, 46). However, the role of GRX1 in other experimental models of PD has not been studied in detail. Recent studies have demonstrated that GRX1 is expressed at lower levels in the substantia nigra and striatum compared to the hippocampus and cerebral cortex (3, 7). Human dopaminergic SK-N-SH cells express very low levels of GRX1, which, as shown here, can be increased by stable expression or adenoviral gene delivery (Figs. 1A and 2A). Stable expression of GRX1 in human dopaminergic cells (Fig. 1A) protects against paraquat induced toxicity (Fig. 1B–1C). More specifically, we observed that GRX1 significantly prevented the loss of mitochondrial activity (Fig. 1B) and cell viability (Fig. 1C) upon

paraquat exposure. To determine if the protective effect of GRX1 overexpression was restricted to paraquat-induced dopaminergic death, we evaluated its role in cell death induced by 6-OHDA, another widely used neurotoxin for experimental PD. As shown in Figure 1D, GRX1 overexpression significantly reduced 6-OHDA toxicity. These results highlight the protective role of GRX1 against distinct experimental models of PD.

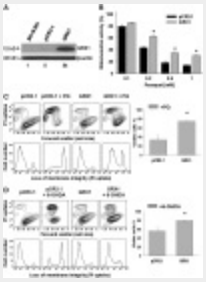

View larger version

FIG. 1. Stable overexpression of GRX1 protects against dopaminergic cell death induced by paraquat and 6-OHDA. Human dopaminergic SK-N-SH cells were stably transfected with empty pCR3.1 vector and pCR3.1 vector encoding human GRX1 **(A)**. In **B–D**, the effect of GRX1 overexpression against cell death induced by a 48 h treatment with paraquat (0.5 m*M* in **C**) or 6-OHDA (50 μ*M*) **(D)** was analyzed by determination of mitochondrial activity **(B)** and cell viability **(C** and **D)**. Mitochondrial activity **(B)** was assessed by measuring the conversion of the tetrazolium salt, MTT. Loss of cell viability or plasma membrane integrity is reflected by the increase in the number of cells with increased PI fluorescence (plots and bar graphs in **C** and **D**). Data in bar graphs represent % of viable cells from paraquat (**C)** and 6-OHDA (**D)** treated cells and are means±SEM of four independent experiments. *$p<0.05$, significant difference between GRX1 and pCR3.1 values. Contour plots and Western blots are representative of 2–4 independent experiments. Numbers in **A** represent the densitometry analysis with respect to SK-N-SH cells normalized to β-actin.

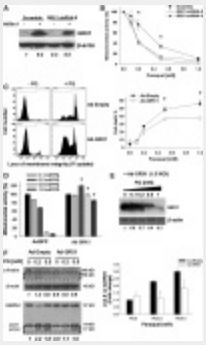

View larger version

FIG. 2. Adenovirus-mediated overexpression of GRX1 and shRNA knock-down regulate dopaminergic cell death induced by paraquat. Overexpression of GRX1 by recombinant adenovirus Ad5CMV-GRX1 (1.5 MOI) and GRX1 knock-down with shRNA lentiviral particles were determined by Western blot **(A)**. The effect of GRX1 overexpression **(C** and **D)** and knock-down **(B)** on the loss of mitochondrial activity **(B** and **D)** and cell death **(C)** induced by paraquat was determined as in Figure 1. In **E**, the effect of paraquat (48 h treatment) on the overexpression of GRX1 induced by Ad5CMV-GRX1 (1.5 MOI) was evaluated. Cleavage of α-fodrin (apoptotic marker) and accumulation of LC3-II (autophagy marker) induced by paraquat were also determined by Western blot in whole cell lysates **(F)**. Control adenovirus contained only the cytomegalovirus promoter (AdEmpty) and/or the green fluorescent protein gene as a reporter (AdGFP). Data in graphs represent means±SEM of four independent experiments. *p<0.05, shRNA4 and 8 vs Scramble **(C)**, or GRX1 *vs.* Empty values **(D)**. Plots in **(C)** represent 0.5 m*M* PQ treatments. Contour plots and Western blots are representative of 3–4 independent experiments. Numbers in blots (*italics*) represent the densitometry analyses with respect to Scramble **(A)**, Ad-GRX1 **(E)**, and Ad-Empty samples **(F)** normalized to β-actin or GAPDH.

To further corroborate the protective role of GRX1 against experimental PD, we used both lentivirus-mediated delivery of shRNA against GRX1 and adenovirus-induced GRX1 overexpression. GRX1 shRNAs (shRNA-4 and shRNA-8) stably expressed in SK-N-SH cells, were able to decrease both basal levels of GRX1 and adenovirus-mediated GRX1 overexpression (Fig. 2A). Knock-down of GRX1 increased paraquat-induced dopaminergic cell death as determined by decreased mitochondrial activity (Fig. 2B). Conversely, overexpression of GRX1 significantly prevented both the decrease in cell viability (Fig. 2C) and the loss of mitochondrial activity upon paraquat exposure (Fig. 2D). Paraquat induced a dose-dependent decrease in the levels of overexpressed GRX1, which explains why a 9-fold increase in GRX1 levels (Fig. 2A) does not completely prevent PQ toxicity

(Fig. 2C).

Paraquat-induced dopaminergic cell death has been associated with the activation of apoptosis and alterations in autophagic pathways (26, 30, 58). Therefore, we wanted to identify the role of GRX1 in regulating distinct signaling pathways. Figure 2F demonstrates that overexpression of GRX1 reduces the cleavage of the selective caspase 3 substrate α-fodrin (15, 41, 87), a reliable marker of apoptosis highly and predominantly expressed in neuronal cells (31, 57). GRX1 also reduced the accumulation of LC3-II as a marker of autophagosome accumulation (Fig. 2F), demonstrating that GRX1 reduces the activation of both apoptotic and autophagic signaling cascades.

Paraquat induces alterations in cellular levels of glutathionylated protein residues

Oxidative stress is associated with increased protein oxidation and alterations in protein glutathionylation. Protein S-glutathionylation refers to the formation of a protein mixed disulfide between the thiol of GSH and the cysteine moiety of a protein (thiol exchange reaction). To examine alterations in protein glutathionylated residues (PSSG) induced by paraquat, whole cell lysates of human dopaminergic cells with or without paraquat treatment were isolated under nonreducing conditions. Figure 3A shows that paraquat induced alterations in overall levels of glutathionylated proteins. Unique protein bands ranging from 37–150 kD were identified, whose signal was reversed when analyzed under reducing conditions (Fig. 3B). In some cases, low concentrations of paraquat induced a slight increase in protein glutathionylation for specific protein bands (broken line rectangle), but higher concentrations were associated with a decrease in PSSG (Fig. 3A and densitometry analysis).

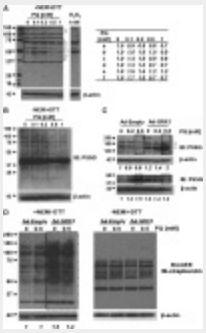

View larger version

FIG. 3. Paraquat-induced alterations in glutathionylated proteins. Whole cell lysates of cells treated with or without paraquat for 48 h were isolated and analyzed under reducing (-NEM/+DTT) and nonreducing (+NEM/-DTT) conditions. In **A** and **B**, protein glutathionylation was assessed using anti-PSSG antibody in samples isolated in the presence or absence of >30 m*M* NEM. In **C**, overexpression of GRX1 was induced via adenoviral transduction (1.5 MOI) as described in Figure 2. **C** represents a composite of two independent Western blot with their corresponding loading controls. In **D**, protein glutathionylation was assessed as previously described in cells labeled with BioGEE (250 μ*M*) 1 h prior to experimental treatments, and glutathionylated proteins were visualized using streptavidin-HRP conjugate. Blots were probed with β-actin to determine equal loading. Blots are representative of at least 3 independent experiments. Numbers in blots (*italics*) represent the densitometry analyses with respect to control **(A,** *table***)**, and Ad-Empty samples **(C** and **D)** normalized to β-actin.

Interestingly, overexpression of GRX1 induced distinct effects on glutathionylated proteins (Fig. 3C). In response to paraquat, a decrease in protein glutathionylation was observed in protein bands around 100–150 kD. GRX1 overexpression increased glutathionylation of these protein bands and this was further increased upon paraquat treatment (Fig. 3C, upper panels a and b). In contrast, paraquat was shown to enhance PSSG of a protein band between 37 and 50 kD (Fig. 3C, lower panel). The glutathionylation of this same protein band was increased by GRX1 itself, but in the presence of paraquat, protein glutathionylation was inhibited. Although it is not possible to determine whether changes in every PSSG band signal are ascribed to single or multiple proteins, these results suggested that alterations in PSSG in response to paraquat and GRX1 overexpression vary according to the molecular identity of the target.

GRX1 activity is usually associated with protein deglutathionylation. To

further confirm the observation that protein glutathionylation was increased by GRX1 overexpression, we used biotinylated GSH (BioGEE) to label the intracellular GSH pool. Figure 3D (left panel) shows that overexpression of GRX1 also increased the levels of glutathionylated proteins when labeled with BioGEE, corroborating our observation that increased GRX1 can stimulate protein glutathionylation. Interestingly, most of the pool of glutathionylated proteins labeled with BioGEE showed an increase in PSSG in response to paraquat treatment, which might imply that labeling protocols for PSSG using either anti-PSSG or BioGEE could actually detect different pools of glutathionylated proteins. It is important to note that modification of the glutathionyl moiety by the bulky biotin molecule is likely to interfere with both enzymatically catalyzed glutathionylation and deglutathionylationation by GRXs (reviewed by Mieyal et al. in Ref. 54). Reducing conditions (+DTT) only partially reversed BioGEE labeling of PSSG residues (Fig. 3D, right panel). Previous studies have shown that some biotin–GSH moieties of glutathionylated proteins are largely resistant to DTT reversal (38).

Paraquat induces the downregulation of flightless-1 homolog protein and the RalBP1-associated Eps domain-containing protein 2

Previous studies have demonstrated the occurrence of protein glutathionylation/deglutathionylation in dopaminergic cells in response to oxidative conditions (52). Glutathionylation of the mitochondrial IDPm was recently reported in the MPTP mouse PD model (47). However, to our knowledge, no other molecular targets have been identified since then in PD models associated with environmental toxicants. We proceeded to identify novel molecular targets for protein glutathionylation/deglutathionylation in dopaminergic cells using mass spectrometry. Paraquat is known to induce

oxidative stress in both mitochondrial and cytosolic compartments (10, 13, 64). We utilized whole cell lysates of untreated dopaminergic cells to immunoprecipitate glutathionylated proteins, which were subsequently analyzed by mass spectrometry in order to identify potential targets for glutathionylation/deglutathionylation upon paraquat exposure. Some of the peptides identified by mass spectrometry analysis corresponded to the actin binding flightless-1 homolog protein (FLI-I, peptide sequence: ACSAIHAVNLR) and the RalBP1-associated Eps domain-containing protein 2 (REPS2/POB1, peptide sequence: SAGSAEQVAPAAAQGGSSRTNCIGKPIGTTSSGHCVV), which have not been previously identified to be subject to oxidative post-translational modification (Fig. 4A, Supplementary Fig. S1; supplementary data are available online at www.liebertonline.com/ars). Supplementary Table 1 lists all the proteins identified in PSSG immunoprecipitates from SK-N-SH cells.

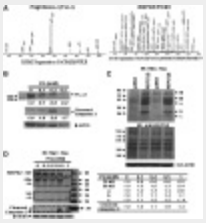

View larger version

FIG. 4. Paraquat toxicity is associated with downregulation of FLI-I and REPS2. (A) Glutathionylated proteins immunoprecipitated with anti-PSSG antibody were processed for mass spectrometry. Samples were digested with trypsin and peptides were subjected to LC/MS/MS analysis using reverse phase chromatography mass spectrometry. Two of the acquired spectrum of peptides identified by mass spectrometry analysis corresponded to FLI-I (ACSAIHAVNLR) and REPS2 SAGSAEQVAPAAAQGGSSRTNCIGKPIGTTSSGHCVV), identified using a human data base (IPI-Human, NCBI). (See Supplementary Fig. S1 for a magnification of the MS spectra). Alterations in the levels of FLI-I, REPS2 and cleaved caspase 3 induced by paraquat were assessed in wild-type **(B)** and stable SK-N-SH overexpressing Myc-His REPS2 **(D)**. In **(C)** and **(D)**, REPS2 protein levels were visualized in stable Myc-His REPS2 overexpressing clones (clone 2 was used in **D**) using anti-myc-tag (*upper panel*) or anti-REPS2 (K-18) (*lower panel*) antibody. a–c labels in **C** and **D** (including the table) represent possible isoforms or degradation products of REPS2. Blots were reprobed with β-actin to corroborate equal loading and are representative of at least 3 independent experiments. Table corresponds to the densitometry analysis of protein bands in **D**. Numbers (*italics*) in **(B)** and **(D)** represent the densitometry analyses with respect to control samples (**D,** *table*) normalized to β-actin.

We next determined the effect of paraquat exposure on protein levels of both FLI-I and REPS2. Paraquat-induced dopaminergic cell death was paralleled by a significant decrease in FLI-I protein levels (Fig. 4B), which corresponded with the activation of apoptosis as shown by the increased cleavage/activation of executioner caspase 3 (Fig. 4B). At high concentrations of PQ and high degree of cell death, no cleaved caspase 3 is detected. This is explained by the well-known observation that active caspase 3 is rapidly degraded by a mechanism that is dependent on the catalytic activity of the active enzyme (81). The effect of paraquat was also determined in stable cells overexpressing REPS2. Four isoforms of REPS2 have been identified: two short isoforms comprising 521 or 522 amino acid residues (58 kD) and two long ones of 659 or 660 residues (78 kD) (6).

Stable overexpression of REPS2 in dopaminergic cells lead to the detection of a 78 kD and 58 kD isoforms (Fig. 4C and 4D). Three other bands at ~50 kD (a), ~32 kD (b), and ~26 kD (c), which could be distinct isoforms or degradation products, were also detected (Fig. 4C and 4D). Detection of basal levels of REPS2 protein was not possible as the commercially available antibody used (K-18, Santa Cruz) did not seem to be specific enough for WB. This was demonstrated by the observation that this antibody was not able to detect myc-tagged REPS2 in our stable cells (Fig. 4C, lower panel), which is recognized by anti-myc-Tag antibody (Fig. 4C, upper panel). Similar to FLI-I, paraquat induced a dose-dependent decrease in the 78 kD isoform (Fig. 4D, broken line rectangle), which paralleled an increase in the other protein bands (Fig. 4D, dotted rectangles and densitometry analysis), suggesting that these might be byproducts of REPS2 degradation. REPS2 degradation was also paralleled by the cleavage/activation of caspase 3 (Fig. 4D, lower panel).

We next determined the effect of GRX1 on protein glutathionylation and expression levels of FLI-I and REPS2. Overexpression of GRX1 was shown to significantly reduce paraquat-induced FLI-I degradation (Fig. 5A, broken line rectangles). Similarly, GRX1 overexpression decreased the degradation of REPS2 (78 kD and 58 kD bands) (Fig. 5B). FLI-I was first immunoprecipitated under nonreducing conditions to determine the alterations in PSSG upon GRX1 overexpression and paraquat treatment. Overexpression of GRX1 was associated with an increase in glutathionylation of FLI-I in the presence of paraquat (Fig. 5C). Reverse-immunoprecipitation with anti-PSSG antibody and blot analysis with anti-FLI-I antibody corroborated the observation that GRX1 overexpression prevented the decrease in glutathionylated FLI-I by paraquat. These results suggest that GRX-1-mediated protein glutathionylation reduces the

degradation of cellular substrates upon oxidative stress induced by paraquat.

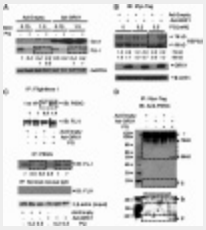

View larger version

FIG. 5. GRX1 regulates protein expression levels and glutathionylation of FLI-I and REPS2. In **(A)** and **(B)**, overexpression of GRX1 (Ad-GRX1) reduced paraquat-induced FLI-I and REPS2 downregulation (*broken line rectangles*). SK-N-SH (**A** and **C**) and cells stably expressing Myc/His REPS2 (**B** and **D**) were infected with Ad-Empty or Ad-GRX1 (1.5 MOI) for 24 h and subsequently treated with paraquat (0.2 m*M* in **A, C** *upper panel*, and **D**) for 48 h. Samples were collected under nonreducing conditions (+NEM/-DTT). In **C** (*upper panel*) and **D**, FLI-I and REPS2 were immunoprecipitated with anti-FLI-I or anti-MycTag antibodies respectively, and then, PSSG were visualized using anti-PSSG antibody. Blot in **(C,** *upper panel***)** was reprobed with anti-FLI-I to corroborate equal levels of immunoprecipitated proteins. In (**C**, *lower panel*), glutathionylated proteins were immunoprecipiated with anti-PSSG antibody and FLI-I levels were visualized using the corresponding antibody. As controls, samples were pre-cleared with Dynabeads coupled with normal mouse IgG. Normal mouse IgG did not pull down FLI-I. Blots are representative of at least 3 independent experiments. Numbers in blots (*italics*) represent the densitometry analyses with respect to Ad-Empty samples [0.15 MOI, upper numbers; and 1.5 MOI lower numbers in **(A)**], normalized to the corresponding loading/input control.

Myc-tagged REPS2 was immunoprecipitated and alterations in PSSG induced by paraquat treatment or GRX1 overexpression were also analyzed. Under nonreducing conditions, the anti-Myc-tag recognized a band >100 kD, which might be either REPS2 complexes or eluted Ig heavy and light chains. Two bands at >80 kD and 58 kD that seem to correspond to the 78 kD and 58 kD isoform were detected using the anti-PSSG antibody, suggesting basal glutathionylation of these isoforms (Fig. 5D, broken lines). Overexpression of GRX1 increased the glutathionylation of the >80 kD protein, while it decreased the PSSG levels in the 58 kD band. Exposure of the GRX1 overexpressing cells to paraquat deglutathionylated the >80 kD isoform, which correlated with an increase in the glutathionylation levels of

the 58 kD isoform. Interestingly, paraquat treatment of GRX1 overexpressing cells also induced an increase in the glutathionylation of the b and c protein bands described in Figure 4 (Fig. 5D, lower panel overexposed). It is important to mention that under nonreducing conditions the migration pattern of the 78 kD and 58 kD isoforms of REPS2 and of their possible degradation products might not correlate with the MW of the protein markers used to identify them. This is because the experimental samples were analyzed under nonreducing conditions (-DTT+NEM), which affect their migration pattern, while recombinant proteins in the protein markers are already reduced (+DTT in the manufacturer's loading buffer).

REPS2 overexpression protects against dopaminergic cell death induced by paraquat

Oxidative stress has been clearly linked to dopaminergic cell death in PD. However, the exact molecular mechanisms by which oxidative stress and redox signaling trigger dopaminergic cell death are unknown. Our results indicate a possible link between degradation of FLI-I and REPS2 proteins and dopaminergic cell death induced by paraquat. Very little is known regarding the role of FLI-I and REPS2 in cellular survival or death. We observed that paraquat treatment induced a decrease in these proteins and this was associated with an increase in the activation of cell death pathways, particularly, the activation of caspases. Thus, we wanted to assess if overexpression of these proteins would modulate dopaminergic cell death induced by paraquat. In two distinct clones of cells stably overexpressing REPS2, paraquat-induced cell death was significantly reduced (Fig. 6A–6B). Figure 6A demonstrates that dopaminergic cell death induced by paraquat, which is observed as an increase in the permeability of the plasma membrane (detected by the uptake of PI) and cell shrinkage (a common

hallmark of apoptotic cell death), was significantly prevented by REPS2 overexpression when compared with cells containing the empty vector (pcDNA). REPS2 overexpression also reduced the cleavage/activation of caspase 3, suggesting a role for REPS2 in regulating apoptotic signaling cascades (Fig. 6B). In contrast to REPS2, overexpression of FLI-I (Fig. 6C–6D) had no effect on paraquat-induced cell death. These results demonstrate for the first time a protective effect of REPS2 against dopaminergic cell death induced by paraquat. Dopaminergic cell death induced by the parkinsonian drugs 6-OHDA (50 μM) or the complex I inhibitors rotenone (4 μM) or MPP^+ (1-methyl-4-phenylpyridinium, 2.5 mM), also used as experimental paradigms of PD, was unaltered by either REPS2 or FLI-I overexpression (data not shown). These are not surprising results as it has been reported that dopaminergic cell death induced by either paraquat, rotenone, MPP^+ or 6-OHDA involves the activation of distinct redox signaling cascades (11, 32, 53, 64, 82). These results also demonstrate that the protective role of REPS2 is specific for paraquat-induced cell death, and that REPS2 overexpression does not impair the overall sensitivity of cells to cell death stimuli.

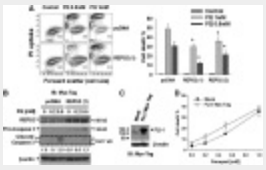

View larger version

FIG. 6. Paraquat-induced dopaminergic cell death is significantly reduced by REPS2/POB1 overexpression. (A) SK-N-SH cells overexpressing empty pcDNA3.1 or Myc-His REPS2 were treated with paraquat for 48 h. Cell death was determined by the loss of plasma membrane integrity (PI uptake) and cell shrinkage as a marker of apoptosis. % of dead cells in **A** (*bar graph*) reflects the number of cells with increased PI fluorescence using two distinct clones overexpressing Myc-His REPS2 (See Fig. 4C). In **B**, paraquat-induced cleavage/activation of caspase 3 in both pcDNA3.1 and REPS2 overexpressing cells was evaluated as explained in Figure 2. In **C** and **D**, cells were transiently transfected with Myc-tagged FLI-I for 24 h prior paraquat treatment. Expression levels of FLI-I were corroborated by Western blot **(C)** and the effect of FLI-I overexpression on paraquat-induced dopaminergic cell death was determined as explained in **A**. Data in **A** (*bar graphs*) and **D** are means±SEM of four independent experiments. *$p<0.05$, significant difference between the corresponding REPS2 and pcDNA3.1 values. Contour plots and western blots are representative of 3–4 independent experiments. Numbers in **B** (*italics*) represent the densitometry analyses of cleaved caspase 3 with respect to pcDNA normalized to β-actin.

To corroborate these results in vivo, C57BL/6 mice were administered two intraperitoneal injections of 10 mg/kg paraquat or PBS every week for 3 consecutive weeks. Animals were analyzed 1 week after the last injection and histological sections of the substantia nigra were stained with anti-TH (tyrosine hydroxylase), anti-PSSG, or anti-REPS2 antibody. Figure 7 demonstrates that paraquat-induced toxicity is associated with a decrease in PSSG (Fig. 7A) and REPS2 (Fig. 7B) levels in the substantia nigra in vivo.

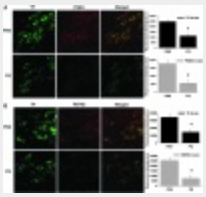

View larger version

FIG. 7. Alterations in PSSG and REPS2 in the substantia nigra of mice treated with paraquat. C57BL/6 mice (8–10 weeks old) were administered two intraperitoneal injections of 10 mg/kg PQ or PBS every week for 3 consecutive weeks. Animals were analyzed 1 week after the last injection and coronal sections of the substantia nigra were stained with anti-TH **(A** and **B)** and anti-PSSG **(A)** or anti-REPS2 **(B)** antibody. Sections were incubated in secondary Alexa 488-anti-rabbit (TH) and Alexa 633-anti-mouse (PSSG and REPS2). Sections were mounted with VectaShield and images were collected on a LSM 5 Exciter confocal scanning fluorescent microscope (20 ×) and Zen 2008 software (Carl Zeiss). Fluorescence intensity analysis was performed using ImageJ (NIH) software. Corrected total cell fluorescence (CTCF) was obtained and expressed as Arbitrary Fluorescence Intensity Units (A.U.).

Discussion

Dopaminergic degeneration in PD is associated with increased oxidative damage. However, the mechanisms by which oxidative stress and redox signaling regulate cell death are unclear. In this study, we demonstrated the protective role of the thiol oxidoreductase GRX1 against the dopaminergic cell death in experimental PD. More specifically, GRX1 was able to significantly reduce dopaminergic cell death induced by paraquat, an environmental pesticide linked by epidemiological studies to an increased risk in PD; and 6-OHDA, a dopaminergic toxin that triggers oxidative damage. Furthermore, we demonstrated that the protective effect of GRX1 is ascribed to an increased glutathionylation that seems to regulate protein degradation during cell death. Finally, we have also identified novel molecular targets for protein glutathionylation, including FLI-I and REPS2; and, for the case of REPS2, we demonstrated its protective effect against dopaminergic cell death induced by paraquat. These results were corroborated in vivo as shown by the decrease in PSSG and REPS2 levels in the substantia nigra of mice treated with paraquat.

Although dopaminergic cell death is a cardinal feature of PD, the mechanisms and pathways involved remain unclear, mainly because in the majority of cases the cause of PD is unknown. A fraction of PD occurrence is related to mutations in genes such as α-synuclein, DJ-1, PINK1, LRRK2, and parkin. However, over 90% of PD occurs most commonly in a sporadic (idiopathic) form without a clearly defined genetic basis, and only a vaguely delineated pathogenesis likely linked to environmental causes. Thus, it is thought that PD arises from the convergence of genetic susceptibility, environmental exposures, and aging, which is the major factor increasing PD risk (37, 84). However, the etiology of PD has yet to be clearly established. Given recent reports strengthening the association between pesticide exposure and increased risk in PD, we decided to study the role of protein glutathionylation and the protective effect of GRX1 in dopaminergic cell death induced by exposure to paraquat, an environmental pesticide whose occupational exposure is linked to PD (23, 80).

To understand the redox signaling events that regulate dopaminergic cell death in experimental PD, we need to identify the molecular targets of oxidative modification. By regulating protein structure and activity, oxidative post-translational modifications regulate a variety of physiological processes. One of the primary targets of oxidation within a protein is the amino acid cysteine, whose thiol side chain is highly sensitive to different types of oxidizing agents. Reversible thiol modification is a major component of the modulation of cell-signaling pathways by ROS. Cysteine oxidation by ROS leads to the formation of the reactive (highly unstable) intermediate cysteine sulfenic acid (PSOH), which, if not reduced, can either participate in disulfide bond formation with GSH (protein glutathionylation) (Fig. 8E) or lead to irreversible oxidation (sulfonic acid) (Fig. 8C and 8G). Protein glutathionylation has also been demonstrated to be

mediated by additional mechanisms (55). For example, PSSG formation might occur by thiol exchange reactions between protein cysteines and glutathione disulfide (GSSG) (Fig. 8A), but this mechanism requires an unusually high redox potential only reported for a limited number of protein targets (55). Protein cysteines and GSH can undergo nitrosylation forming protein-SNO and (S-)nitrosoglutathione (GSNO) and biochemical studies demonstrate the potential of GSNO to promote protein S-glutathionylation (55). Paraquat generates oxidative stress by an increased accumulation of reactive species such as superoxide anion ($\bullet O_2^-$) and hydrogen peroxide (H_2O_2), which parallel a decrease in cellular GSH levels and increased generation of GSSG (44). Interestingly, we observed distinct effects of paraquat exposure on PSSG levels. In some cases, paraquat toxicity was paralleled by a decrease in PSSG residues (Fig. 3A and 3C). This might be associated with: 1) a depletion of intracellular GSH preventing its reaction with PSOH residues and the formation of PSSG residues (Fig. 8C–8E); and 2) the hyperoxidation of PSOH residues (Fig. 8G). In some other protein bands, paraquat induced an increase in PSSG levels (Fig. 3A and C), which might be mediated by the increased accumulation of GSSG and its reaction with protein targets with high redox potential (Fig. 8A). These results demonstrate the occurrence of distinct glutathionylation/deglutathionylation mechanisms induced by paraquat that could be related to distinct protein localization, surrounding redox environment (availability of GSH or GSSG), and the nature of the reactive species involved.

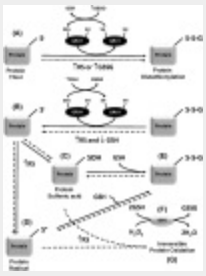

View larger version

FIG. 8. Proposed mechanism by which paraquat-induced oxidative stress and GRX1 might regulate protein glutathionylation and deglutathionylation distinctively. Protein glutathionylation has been demonstrated to occur by a variety of mechanisms, reviewed in (55, 88). **(A)** PSSG formation might occur by thiol exchange reactions between protein cysteines and GSSG, but this mechanism requires unusually high redox potential. Interestingly, under oxidizing conditions (low GSH/GSSG ratio) GRX1 can use GSSG to promote PSSG formation. Paraquat-induced↑RS might enhance GRX1-mediated glutathionylation by increasing the GSSG pool (*dotted line*). **(B)** Under reducing conditions, GRX1 utilizes the reducing power of GSH to catalyze protein deglutathionylation. Paraquat-induced reactive species (↑ RS) formation might prevent GRX1-mediated deglutathionylation by depletion of intracellular GSH content (*broken lines*). On the other hand, two (H_2O_2, •$ONOO^-$) or one-electron (•O_2^-) cysteine oxidation by RS leads to the formation of reactive intermediates including cysteine sulfenic acids (PSOH) **(C)** and protein thiyl radicals (PS•) **(D)**, respectively, which can participate in disulfide bond formation with GSH leading to PSSG formation **(E)**. In addition, GS• generation by oxidative stress has been shown to lead to PSSG formation catalyzed by GRXs (not depicted here). This is another potential mechanism by which GRX1 overexpression might increase protein glutathionylation upon paraquat exposure. Paraquat-induced RS formation and GSH depletion mediated by increased activation of glutathione peroxidase (GPX) (*broken lines)* might enhance cysteine oxidation and also prevent/reverse cysteine glutathionylation leading to their irreversible oxidation **(G)**. Thus, glutathionylation/deglutathionylation depends on the spacial localization of the targeted protein, surrounding redox environment, the nature of the RS involved and expression levels of GRXs **(F)**.

Protein glutathionylation linkages are removed by changes in the intracellular GSH/GSSG balance and/or the activities of GRX enzymes. GRXs are oxidoreductases that under reducing conditions utilize the reducing power of GSH to catalyze protein deglutathionylation (reduction of mixed disulfides) (Fig. 8B) (55). Interestingly, formation of PSSG has also been observed as a result of thiyl radical formation by reactive species (protein thiyl [PS●] and glutathionyl [GS●] radicals), which can be

catalyzed by GRXs (29, 63, 78). This suggests that protein glutathionylation/deglutathionylation catalyzed by GRX1 depends upon the redox environment of the cell, with the potential to act as a glutathionylating enzyme under oxidative stress, and as a deglutathionylase under reducing conditions (high GSH availability) or when the oxidative stress subsides (9, 55). Previous studies have demonstrated the occurrence of protein glutathionylation/deglutathionylation in dopaminergic cells and experimental PD models, but these observations have been restricted to the mitochondria. In this study, we demonstrated that GRX1 has the ability to promote both glutathionylation and deglutathionylation in dopaminergic cells, and this was modulated by the oxidative stress induced by paraquat. For example, PSSG levels were decreased by paraquat exposure and overexpression of GRX1 not only increased PSSG formation by itself, but this effect was enhanced by paraquat (see Fig. 3C upper panel and 3D). The glutathionylating activity of GRX1 under these circumstances might be ascribed to the increased levels of oxidized GSH (GSSG or GS●) acting as substrate for GRX1 (Fig. 8A). In other cases, an increase in PSSG was induced by either paraquat or GRX1 overexpression, and this was reversed by both paraquat and high GRX1 levels (see Fig. 3C, lower panel), which could be associated with inactivation or degradation of GRX1 by oxidative stress. These results support the idea that paraquat-induced alterations in PSSG are determined by distinct variables, including the susceptibility of the protein (redox potential and availability of cysteine residues), the redox environment surrounding the protein, the generation of pro-oxidant conditions, and possibly the compartmentalization of these events.

GRX1 appears to be expressed at lower levels in the substantia nigra and striatum compared to other brain areas (3, 7), which suggests that the low expression levels of this thiol transferase might render dopaminergic cells

more susceptible to oxidative stress. GRX1 and GRX2 have been suggested to play a protective role against dopamine toxicity in neuronal cells (16, 17). Downregulation of GRX1 itself has been shown to induce a decrease in complex I activity, mitochondrial membrane potential, DJ-1 loss (a putative gene recessively linked to early onset of PD), translocation of DAXX (a death-associated protein), and cell death (46, 68, 69). Mieyal's research group recently reported that levodopa (L-DOPA), a dopamine precursor used in the clinical treatment for PD, directly inactivates GRX1 and induces dopaminergic cell death by activation of the apoptosis signaling kinase 1 (ASK-1) (66, 67). On the other hand, downregulation of mitochondrial GRX2 has been shown to disrupt iron–sulfur center biogenesis and complex I activity in dopaminergic cells, while its overexpression protects against MPTP-induced toxicity (45, 48). In mouse embryonic fibroblasts, lack of GRX1 is associated with increased sensitivity to paraquat toxicity (36). However, the protein target(s) subject to either glutathionylation/deglutathionylation that might mediate the protective effects of GRXs in dopaminergic cells have not been elucidated. It is important to notice that overexpression of GRX1 only partially protects dopaminergic cells. This is explained by the observation that paraquat induced a decrease in the levels of overexpressed GRX1. In addition, GRX1 requires GSH/GSSG for its glutathionylating/deglutathionylating activity, and paraquat toxicity is associated to GSH depletion by its oxidation to GSSG and possibly, by GSSG extrusion outside of the cell, both of which might alter GRX1 activity (Fig. 8A and 8B).

Paraquat triggers a dose-dependent decrease in cell viability and mitochondrial activity (Figs. 1B, 2B, and 2C). Overexpression or knock-down of GRX1 regulate PQ-induced cell death irrespective to the concentration used. However, alterations in PSSG levels presented distinct

patterns. In some cases, paraquat induced a dose-dependent decrease in PSSG residues (Fig. 3A, protein band a). In other cases (Fig. 3A, protein bands c, d and f), lower concentrations of paraquat (0.1 and 0.2 mM) induced an initial increase in PSSG residues that were deglutathionylated in response to higher paraquat doses (0.5 and 1 mM). This biphasic behavior might be explained by the presence of distinct protein targets with distinct redox potentials in WB bands or by the distinct susceptibility (distinct pKa values) of different cysteine residues within protein targets subject to glutathionylation/deglutathionylation or hyperoxidation.

GRX1 has been shown to protect against oxidative stress by regulation of pro-apoptotic signaling proteins such as the ASK-1 (77). Although distinct proteins both in the cytosolic and mitochondrial compartments have been reported to be the target for glutathionylation (39, 55), very few glutathionylated proteins have been identified in dopaminergic cells in experimental PD and these have been restricted to the mitochondria. Mitochondrial protein deglutathionylation has been reported in response to oxidative stress in dopaminergic cells (56), while increased IDPm glutathionylation was reported in the MPTP mouse model (47). Paraquat is known to induce oxidative stress in both mitochondria and cytosolic compartments (10, 13, 64), thus, we wanted to identify novel targets of protein glutathionylation using a human dopaminergic cell line as a robust experimental model for protein analysis by mass spectrometry. We were able to identify two new proteins, which to our knowledge, have not been reported previously to be subject to redox modifications. These two protein targets, FLI-I and REPS2, were degraded upon paraquat treatment and this was paralleled by executioner caspase activation. GRX1 overexpression was able to significantly reduce the degradation of FLI-I and REPS2, and this was associated with reversal in paraquat-induced

glutathionylation/deglutathionylation of these enzymes, suggesting that under oxidative conditions, GRX1 might exert a protective effect against the degradation of proteins by modulation of glutathionylation/deglutathionylation residues. For example, it has been proposed that PSSG prevents critical cysteine residues from overoxidation (55). Our next step would be to evaluate if glutathionylation/deglutathionylation of proteins such as FLI-I and REPS2 leads to their degradation by cysteine hyperoxidation.

Actin is a well-known substrate of glutathionylation. Previous reports have demonstrated that actin glutathionylation occurs via spontaneous oxidation of a cysteinyl residue to a PSOH that readily reacts with GSH (20, 43). Actin deglutathionylation is mediated by GRX1 and regulates its polymerization induced by growth factor stimulation (18, 85, 86). FLI-I is a member of the gelsolin superfamily of proteins, which contains another six members: villin, adseverin, capG, advillin, supervillin, and gelsolin. In addition to their respective role in actin filament remodeling, these proteins have some specific and apparently non-overlapping roles in several cellular processes, including cell motility, control of apoptosis, and regulation of phagocytosis (75). Gelsolin-related actin binding proteins contain a triple repeat of a 125–150 amino acid residue actin-binding subdomain, referred to as S1, S2, or S3. In most members, including FLI-I, there are two copies of this triple repeat region, yielding a six-subdomain protein (S1–S6). The FLI-I protein also contains a N-terminal leucine-rich repeat region involved in protein–protein interactions. FLI-I is the only member of the gelsolin superfamily that is essential for mouse development, as disruption of the mouse homologue fliih gene results in a rapid degeneration of the embryo (4). Knock-down of FLI-I increases apoptosis induced by cytokine withdrawal, suggesting that FLI-I is a survival factor (90). Recently, it was demonstrated

the ability of FLI-I to bind and inhibit pro-inflammatory caspase 1 (51). Here we demonstrated that FLI-I is downregulated during paraquat-induced dopaminergic cell death, and this was paralleled by increased executioner caspase 3 activation, but whether caspases mediate FLI-I downregulation or FLI-I regulates executioner caspase activation requires further research. Importantly, downregulation of FLI-I was significantly prevented by its GRX1-mediated glutathionylation. Another report demonstrated a direct interaction of nucleoredoxin, a member of the thioredoxin family of protein oxidoreductases, with FLI-I, but this seemed to be unaffected by oxidative stress and independent of the two catalytically active cysteine residues (34). Overexpression of FLI-I did not prevent paraquat-induced toxicity; however, further studies are required to clearly determine its role in dopaminergic cell death as both its expression levels and redox status (glutathionylation) seem to be altered during oxidative stress-induced by paraquat.

REPS2/POB1 is homologous in sequence and domain structure to REPS1. The Reps (Related to Eps15) proteins contain a domain homologous to Eps15, which has been identified in 11 human proteins. REPS2 regulates the signaling processes by altering the localization of a molecule within the cell, thus linking signaling and intracellular trafficking. Four isoforms of REPS2 have been identified. Two short (58 kD) isoforms and two long (78 kD) ones (6). mRNA and protein analysis demonstrated that REPS2 is predominantly expressed in the central nervous system as compared to other tissues (33, 40), being particularly enriched in neuronal populations (33, 49). REPS2 has been shown to regulate glutamate receptor endocytosis (33), but no further studies have addressed its role in neuronal function. REPS2 also regulates cell death pathways. In cancer cell lines, increased expression of REPS2 is associated with increased apoptosis (59, 76, 91). Similar to

FLI-I, paraquat-induced toxicity was associated with downregulation of REPS2, which was significantly reduced by GRX1 overexpression. More extensive studies are required to identify the specific cysteines in both FLI-I and REPS2 that are subject to protein oxidation, as well as the exact mechanisms by which these cellular substrates regulate paraquat-induced dopaminergic cell death.

In summary, we have demonstrated for the first time, the protective role of GRX1 and protein glutathionylation against dopaminergic cell death in the experimental PD models of paraquat and 6-OHDA. Furthermore, we demonstrate that the protective effect of GRX1 might be ascribed to alterations in glutathionylation/deglutathionylation of cellular protein targets, which could potentially protect them from hyperoxidation and/or degradation during cell death. Finally, we have identified novel molecular targets of protein glutathionylation, including FLI-I and REPS2; and for the case of REPS2, we have demonstrated its protective effect against dopaminergic cell death induced by experimental PD.

Materials and Methods

Cell culture and treatments

Human dopaminergic neuroblastoma cells (SK-N-SH) were obtained from the American Type Culture Collection (ATCC; Manassas, VA). Cells were cultured in DMEM/F12 medium containing 10% fetal bovine serum, 100 units/ml penicillin-streptomycin in a humidified 37°C incubator with 5% CO_2. Cell culture reagents were obtained from Thermo Scientific/Hyclone (Logan, UT) or Invitrogen/GIBCO (Carlsbad, CA). Cells were treated with paraquat (1,1′-dimethyl-4,4′-bipyridinium dichloride), 6-hydroxydopamine

hydrochloride (6-OHDA), 1-methyl-4-phenylpyridinium iodide (MPP^+), and rotenone (SIGMA-Aldrich, St. Louis, MO) to induce cell death. 6-OHDA was prepared in water containing ascorbic acid (0.02%) to prevent its oxidation.

Plasmids, stable and transient transfections

pCR3.1 vector and pCR3.1 vector expressing human GRX1 were kind gifts of Dr. Marjorie F. Lou (University of Nebraska, Lincoln, NE) (89). pEF-BOS-Myc-tagged FLI-I and pcDNA3.1/Myc-His REPS2/POB1 expression vectors were kindly provided by Dr. Hiroaki Miki (Laboratory of Intracellular Signaling, Institute for Protein Research, Osaka University) (34) and Dr. Luisa Castagnoli (University of Rome Tor Vergata) (83), respectively. Plasmids were linearized with ScaI (pCR3.1) and PvuI (pcDNA3.1) restriction enzymes and transfected into SK-N-SH cells using FuGENE HD reagent (Promega, Madison, WI). Stable cells overexpressing REPS2 were selected in complete medium containing 0.3 mg/ml geneticin. Transient expression of Myc-tagged FLI-I was performed with FuGENE (4.5 FuGENE: 1 DNA).

Knockdown of GRX1

Knockdown experiments were designed according to previous studies (65). Cells were stably transduced with mission short hairpin small interference RNA (shRNA) lentiviral particles (Sigma-Aldrich). Cells were infected with the lentiviral pLKO.1 shRNA vectors (Sigma Mission shRNA library) TRCN0000036224 / NM_002064.1-229s1c1, named shRNA-4, Sequence: CCGGCGAGTCTTTATTGGTAAAGATCTCGA GATCTTTACCAATAAAGACTCGTTTTTG; TRCN0000036225/NM_002064.1-111s1c1, named shRNA-5, Sequence:

CCGG CCTCAGTCAATTGCCCATCAACTCGAGTTGATGGGC AATTGACTGAGGTTTTTG; TRCN0000036226/NM_002064.1-260s1c1, named shRNA-6, Sequence: CCGGGATGCAG TGATCTAGTCTCTTCTCGAGAAGAGACTAGATCACT GCATCTTTTTG; TRCN0000036227 / NM_002064.1-172s1c1, named shRNA-7, Sequence: CCGGCACACTAACGAGAT TCAAGATCTCGAGATCTTGAATCTCGTTAGTGTGTTT TTG; and TRCN0000036228 / NM_002064.1-242s1c1, named shRNA-8, Sequence: CCGGGTAAAGATTGTATAGGCGG ATCTCGAGATCCGCCTATACAATCTTTACTTTTTG; and selected in medium containing 3 µg/ml puromycin after 48 h post-transfection. As control, we used a non-target shRNA pLKO.1 (SHC002, Sequence: CCGGCAACAAGATGAAGAGC ACCAACTCGAGTTGGTGCTCTTCATCTTGTTGTTTTT) coding for the puromycin resistance gene and containing a sequence that should not target any known human gene (scramble), but will engage with the RNA-induced silencing complex (RISC). All lentiviruses were packaged in HEK293T cells according to established protocols (8). Briefly, HEK293T cells were transiently transfected with pMD2G, psPAX2, and transfer vector containing the shRNA sequence using Lipofectamine 2000. Supernatant was collected 48 h post-transfection and concentrated by centrifugation at 50,000 g for 2 h. The pellets were resuspended in PBS and used for infection. Only shRNA-4 and shRNA-8 decreased GRX1 basal and overexpression levels (data not shown).

Recombinant adenoviral vectors

The replication-deficient recombinant adenovirus (E1 deletion) Ad5CMV-GRX1 containing the transgene for human GRX1 under the control of the

CMV promoter was kindly provided by Dr. J.J. Mieyal of Case Western Reserve University, Cleveland, OH (72). Control adenoviruses containing only the cytomegalovirus promoter (AdEmpty) or the green fluorescent protein gene as a reporter (AdGFP) were used as controls. Adenoviruses were amplified in HEK293T cells according to established protocols (8). HEK293T cells were infected and then harvested when cytopathic effect was observed (CPE). Pellet and supernatant were harvested, three rounds of freeze/thaw were performed to release viral particles, and debris was removed by centrifugation. Viruses in the supernatant were titered using a modification of the end-point dilution assay. SK-N-SH cells were infected with adenoviral vectors at a multiplicity of infection (MOI) of 0.15–15 and treated with experimental conditions 24 h post-infection.

Measurement of mitochondrial activity (cytotoxicity assay)

Mitochondrial activity was assessed as a marker of cytotoxicity by measuring the conversion of the tetrazolium salt, MTT, to formazan. After treatment, cells were incubated with MTT (0.5 mg/ml, Sigma) at 37°C. Then, lysis buffer (10% SDS in 0.01 N HCl) was added and samples were incubated until complete lysis. Absorbance was measured at 570 nm and results were expressed as % of mitochondrial activity with respect to the control (untreated) cells.

Analysis of cell viability by FACS

After treatment, floating and attached cells were collected. Loss of cell viability was determined by propidium iodide uptake (PI, Sigma) as a marker for plasma membrane integrity loss using flow cytometry (FACS, Fluorescence Activated Cell Sorting). PI was detected in FL-3 (488 nm excitation, 695/40 nm emission) or L2-4 (561 nm excitation and 615/25 nm

emission) in a BD FACScaner (BD Biosciences, San Diego, CA) or BDFACSort (Cytek-DxP-10 upgrade), and data were analyzed with CellQuest or FlowJo 7.6.5 software.

Western blotting under reducing and nonreducing conditions

After treatments, cells were collected in RIPA buffer (25 mM Tris.HCl, pH 7.6, 150 mM NaCl, 1% Triton X-100, 1% sodium deoxycholate, 0.1% SDS) supplemented with Halt Protease Inhibitor (Thermo/Pierce, Rockford, IL). To normalize protein concentration, protein content from whole cell lysates was determined via the bicinchoninic acid method (BCA, Thermo/Pierce). NuPAGE LDS sample buffer (Invitrogen) was added to the samples with (reducing conditions) or without reducing agent (nonreducing conditions) and heated for 10 min at 70°C. Samples were separated on NuPAGE 4%–12% Bis-Tris gels (Invitrogen) with (reducing conditions) or without antioxidant (nonreducing conditions), and transferred to nitrocellulose membranes (Whatman/GE Life Sciences, West Grove, PA) using NuPAGE transfer buffer and a TE70X semi-dry blotter (Hoefer, San Francisco, CA). Membranes were probed with the appropriate antibodies: anti-GRX1 (Abcam, Cambridge, MA); anti-α-fodrin, anti-cleaved caspase 3 (ASP175) (Cell Signaling Technology, Danvers, MA), anti-LC3B (SIGMA), anti-glutathione (anti-PSSG, Virogen,Watertown, MA); anti-GAPDH (Cell Signaling Technology), anti-β-actin (Sigma), anti-FLI-I (Bethyl Laboratories, Montgomery, TX), anti-Myc Tag (clone 4A6, EMD/Millipore) and anti-REPS2 (Santa Cruz Biotechnology, Santa Cruz, CA) at 4°C overnight. Peroxidase conjugated secondary anti-rabbit or anti-mouse antibodies (1:5000, GE Life Sciences, Abcam or Thermo/Pierce or Cell Signaling Technology) were used, and bands were detected using ECL Western blotting substrate (GE Life Sciences or Thermo/Pierce). To identify

alterations in protein glutathionylation, cells were collected in RIPA buffer containing >30 mM N-ethylmaleimide (NEM) (Sigma-Aldrich) to irreversibly block free thiols and minimize further thiol–disulfide exchange, and samples were analyzed under nonreducing conditions as explained above. The addition of NEM stabilizes PSSG by preventing the transfer of GSH from one protein thiol to another. NEM blocks exposed thiols that have not been glutathionylated and also thiols that become exposed by denaturation of the protein during sample processing. 10 mM NEM was supplemented into the blocking buffer after the proteins were transferred to nitrocellulose membranes. Glutathionylated proteins were visualized using an anti-glutathionylated (anti-PSSG) antibody, which is raised against GSH connected by a thioether bond through a linker to a keyhole limpet hemocyanin.

Immunoprecipitation

Cells were collected and lysed in RIPA buffer. 300–500 µg protein for each sample were pre-cleared with either Trueblot mouse IgG beads (eBIOSCIENCE, San Diego, CA), or protein A Dynabeads (Invitrogen) coupled to normal rabbit or mouse IgG for 1 h at 4°C, and then washed in buffer containing 20 mM Tris-HCl, pH 7.5, 137 mM NaCl, 2 mM EDTA, and 10% glycerol. Then, immunoprecipiation was performed by incubating protein samples for 1 h at 4°C with Dynabeads bound to the corresponding primary antibody (0.2–2 µg per sample) using the Dynal Magnetic Particle Concentrator (Invitrogen). Proteins were eluted with glycine elution buffer (100 mM glycine, pH 2.5) for mass spectrometry analysis or NuPAGE LDS sample buffer with or without (PSSG immunoprecipitation) reducing agent for Western immunoblot. For immunoprecipitation using the anti-PSSG antibody, free GSH was initially removed from protein samples with a

Nanosep 3K centrifugal device (Pall Life Science, Port Washington, NY) at 14000 g for 5 min.

Analysis of glutathionylated proteins using biotinylated GSH ester

This method was modified from previously described protocols (12, 79). Biotinylated GSH ester (BioGEE) was prepared by mixing equal volumes of 25 mM sulfo-NHS-biotin (Thermo/Pierce) with 25 mM GSH ethyl ester (Sigma) in 50 mM $NaHCO_3$ at pH 8.5, followed by the addition of 125 mM NH_4HCO_3 at pH 8.5. To terminate the reaction, 1.25 M NH_4HCO_3 was added to quench the remaining biotinylation reagents at 5-fold molar excess of the starting sulfo-NHS-biotin concentration. Cells were pre-incubated in serum-free media with BioGEE (250 μM) for 1 h and then treated with the corresponding experimental conditions. Then, cells were collected, washed and lysed in a nondenaturing lysis buffer (TrisHCl 25 mM, pH 7.4, NaCl 150 mM, $MgCl_2$ 5 mM, 1% NP-40) containing 10 mM NEM. After sonication and centrifugation, the samples were analyzed under nonreducing conditions, and glutathionylated proteins were visualized using streptavidin–HRP conjugate (Thermo/Pierce).

Mass spectrometry analysis and protein identification

Glutathionylated proteins immunoprecipitated with anti-PSSG antibody were immediately neutralized with 1 M Tris.HCl (pH 8), and processed for mass spectrometry. Samples were initially buffer exchanged with 100 mM ammonium bicarbonate buffer pH 8.0, reduced using DTT and alkylated using iodoacetamide. Samples were then digested using Trypsin (Roche) and subsequently dried using Speed Vac concentrators. Peptides were subjected to LC/MS/MS analysis using reverse phase chromatography mass spectrometry. The LC/MS/MS analysis was carried out using a Dionex U

3000 nano LC unit. Sample loading on the monolithic trap column was conducted using a micro pump. The desalted peptides were eluted and separated on a C 18 Pep Map column (75 μm I.DX15 cm, 3 μm) applying an acetonitrile gradient (ACN plus 0.1% formic acid) and introduced into the mass spectrometer using the nano spray source. The LCQ Fleet mass spectrometer (Thermo Electron Corporation) operates with the following parameters: nano spray voltage (2.0 kV), heated capillary temperature 200C, full scan m/z range 400–2000. The LCQ was operated in data dependant mode with 4 MS/MS spectra for every full scan, 5 microscan averaged for full scans and MS/MS scans in CID mode. The acquired spectrum was searched against human data base (IPI-Human, NCBI) for sequence analysis using MASCOT data base analysis software.

In vivo mouse model of paraquat toxicity

C57BL/6 mice (8–10 weeks old) (Jackson Labs) were administered two intraperitoneal injections of 10 mg/kg PQ or PBS every week for 3 consecutive weeks. Animals were analyzed 1 week after the last injection. Mice were perfused intracardially with 4% paraformaldehyde (PFA) in 0.1 M sodium phosphate buffer (pH 7.4). Brains were removed, post-fixed for 24 h in 4% PFA and cryoprotected with 30% sucrose. Frozen brains were cut into 30 μm coronal sections using a sliding microtome at −16°C, and stored in PBS at 4°C until the immunohistochemical procedure. Endogenous peroxidase activity was inactivated. Sections were blocked with 10% normal horse serum (GIBCO) and incubated 48 h with rabbit anti-TH antibody (Calbiochem, EMD/Millipore) anti-REPS2 or anti-PSSG at 4°C. After rinsing, sections were incubated in secondary Alexa 488-anti-rabbit or Alexa 633-anti-mouse (Molecular Probes/Invitrogen) for 1 h at RT. Sections were mounted with VectaShield (Vector Laboratories, Burlingame, CA).

Images were collected on a LSM 5 Exciter confocal scanning fluorescent microscope (20×) and Zen 2008 software (Carl Zeiss).

Statistical analysis

All experiment replicas were independent and performed on separate days. Collected data were analyzed according to statistical criteria by using paired or unpaired t-test, one-way ANOVA or two-way ANOVA, and the appropriate parametric or nonparametric normality post-test using a SIGMA-PLOT/STAT package. A probability value of $p<0.05$ was considered as statistically significant. Data were plotted as mean values of at least three independent experiments±standard error of the mean (SEM) using the same statistical package for data analysis. Flow cytometry plots and Western blots presented were representative of at least three independent experiments. Confocal image analysis and densitometry analysis of immunoblots were performed using ImageJ (NIH) v3.91 software (http://rsb.info.nih.gov/ij). Corrected total cell fluorescence (CTCF) was obtained with the next formula CTCF=Integrated Density – (Area of selected cell X Mean fluorescence of background readings).

Supplementary Material

Open In Web Browser

Acknowledgments

This work was supported by the National Institutes of Health Grant P20RR17675 Centers of Biomedical Research Excellence (COBRE), the Research Council Interdisciplinary Grant, and the Life Sciences Grant Program of the University of Nebraska-Lincoln. LZF received a Post-

doctoral Fellowship from the National Council of Science and Technology (CONACYT 211456) of Mexico. We would like to thank Dr. Charles A. Kuszynski and Zhi Hong Gill at the Nebraska Center for Virology for their help in the flow cytometry analyses.

Author Disclosure Statement

The authors declare no competing financial interests.

Abbreviations Used

ASK-1 apoptosis signal-regulating kinase 1
BioGEE biotinylated GSH ester
DTT dithiothreitol
FLI-I Flightless I
GPX glutathione peroxidase
GRX glutaredoxin
GS• glutathionyl radical
GSH glutathione
GSNO nitrosoglutathione
GSSG glutathione disulfide
H_2O_2 hydrogen peroxide
IDPm NADP(+)-dependent isocitrate dehydrogenase
MPTP 1-methyl-4-phenyl-1,2,3,6-tetrahydropyridine
NEM N-ethylmaleimide
$\bullet O_2^-$ superoxide anion
$\bullet ONOO^-$ peroxynitrite
PD Parkinson's disease
PS• protein thiyl radicals

PSOH protein sulfenic acids

PSSG protein glutathionylated residues

REPS2 RalBP1-associated Eps domain-containing protein 2

ROS reactive oxygen species

SH thiol group

SNpc substantia nigra pars compacta

References

1. Alam ZI, author; Daniel SE, author; Lees AJ, author; Marsden DC, author; Jenner P, author; Halliwell B, author. A generalised increase in protein carbonyls in the brain in Parkinson's but not incidental Lewy body disease. J Neurochem. 69:1326–1329. 1997;[PubMed]
2. Alam ZI, author; Jenner A, author; Daniel SE, author; Lees AJ, author; Cairns N, author; Marsden CD, author; Jenner P, author; Halliwell B, author. Oxidative DNA damage in the

parkinsonian brain: An apparent selective increase in 8-hydroxyguanine levels in substantia nigra. J Neurochem. 69:1196–1203. 1997;[PubMed]

3. Aon-Bertolino ML, author; Romero JI, author; Galeano P, author; Holubiec M, author; Badorrey MS, author; Saraceno GE, author; Hanschmann EM, author; Lillig CH, author; Capani F, author. Thioredoxin and glutaredoxin system proteins-immunolocalization in the rat central nervous system. Biochim Biophys Acta. 1810:93–110. 2011;[PubMed]
4. Archer SK, author; Claudianos C, author; Campbell HD, author. Evolution of the gelsolin family of actin-binding proteins as novel transcriptional coactivators. Bioessays. 27:388–396. 2005;[PubMed]
5. Ascherio A, author; Chen H, author; Weisskopf MG, author; O'Reilly E, author; McCullough ML, author; Calle EE, author; Schwarzschild MA, author; Thun MJ, author. Pesticide exposure and risk for Parkinson's disease. Ann Neurol. 60:197–203. 2006;[PubMed]
6. Badway JA, author; Baleja JD, author. Reps2: A cellular signaling and molecular trafficking nexus. Int J Biochem Cell Biol. 43:1660–1663. 2011;[PubMed]
7. Balijepalli S, author; Tirumalai PS, author; Swamy KV, author; Boyd MR, author; Mieyal JJ, author; Ravindranath V, author. Rat brain thioltransferase: Regional distribution, immunological characterization, and localization by fluorescent in situ hybridization. J Neurochem. 72:1170–1178. 1999;[PubMed]
8. Barde I, author; Salmon P, author; Trono D, author. Production and titration of lentiviral vectors. Curr Protoc Neurosci. . Chapter 4: Unit 4. 21:2010;
9. Beer SM, author; Taylor ER, author; Brown SE, author; Dahm CC, author; Costa NJ, author; Runswick MJ, author; Murphy MP, author. Glutaredoxin 2 catalyzes the reversible oxidation and glutathionylation of mitochondrial membrane thiol proteins: Implications for mitochondrial redox regulation and antioxidant DEFENSE. J Biol Chem. 279:47939–47951. 2004;[PubMed]
10. Castello PR, author; Drechsel DA, author; Patel M, author. Mitochondria are a major source of paraquat-induced reactive oxygen species production in the brain. J Biol Chem. 282:14186–14193. 2007;[PubMed]
11. Choi WS, author; Yoon SY, author; Oh TH, author; Choi EJ, author; O'Malley KL, author; Oh YJ, author. Two distinct mechanisms are involved in 6-hydroxydopamine- and MPP+-induced dopaminergic neuronal cell death: Role of caspases, ROS, and JNK. J Neurosci Res. 57:86–94. 1999;[PubMed]
12. Clavreul N, author; Adachi T, author; Pimental DR, author; Ido Y, author; Schoneich C, author; Cohen RA, author. S-glutathiolation by peroxynitrite of p21ras at cysteine-118

mediates its direct activation and downstream signaling in endothelial cells. FASEB J. 20:518–520. 2006;[PubMed]

13. Cocheme HM, author; Murphy MP, author. Complex I is the major site of mitochondrial superoxide production by paraquat. J Biol Chem. 283:1786–1798. 2008;[PubMed]
14. Costello S, author; Cockburn M, author; Bronstein J, author; Zhang X, author; Ritz B, author. Parkinson's disease and residential exposure to maneb and paraquat from agricultural applications in the central valley of California. Am J Epidemiol. 169:919–926. 2009; [PubMed]
15. Cryns VL, author; Bergeron L, author; Zhu H, author; Li H, author; Yuan J, author. Specific cleavage of alpha-fodrin during Fas- and tumor necrosis factor-induced apoptosis is mediated by an interleukin-1beta-converting enzyme/Ced-3 protease distinct from the poly(ADP-ribose) polymerase protease. J Biol Chem. 271:31277–31282. 1996;[PubMed]
16. Daily D, author; Vlamis-Gardikas A, author; Offen D, author; Mittelman L, author; Melamed E, author; Holmgren A, author; Barzilai A, author. Glutaredoxin protects cerebellar granule neurons from dopamine-induced apoptosis by activating NF-kappa B via Ref-1. J Biol Chem. 276:1335–1344. 2001;[PubMed]
17. Daily D, author; Vlamis-Gardikas A, author; Offen D, author; Mittelman L, author; Melamed E, author; Holmgren A, author; Barzilai A, author. Glutaredoxin protects cerebellar granule neurons from dopamine-induced apoptosis by dual activation of the ras-phosphoinositide 3-kinase and jun n-terminal kinase pathways. J Biol Chem. 276:21618–21626. 2001;[PubMed]
18. Dalle-Donne I, author; Giustarini D, author; Rossi R, author; Colombo R, author; Milzani A, author. Reversible S-glutathionylation of Cys 374 regulates actin filament formation by inducing structural changes in the actin molecule. Free Radic Biol Med. 34:23–32. 2003; [PubMed]
19. Dalle-Donne I, author; Rossi R, author; Colombo G, author; Giustarini D, author; Milzani A, author. Protein S-glutathionylation: A regulatory device from bacteria to humans. Trends Biochem Sci. 34:85–96. 2009;[PubMed]
20. Dalle-Donne I, author; Rossi R, author; Giustarini D, author; Colombo R, author; Milzani A, author. Actin S-glutathionylation: Evidence against a thiol-disulphide exchange mechanism. Free Radic Biol Med. 35:1185–1193. 2003;[PubMed]
21. Danielson SR, author; Andersen JK, author. Oxidative and nitrative protein modifications in Parkinson's disease. Free Radic Biol Med. 44:1787–1794. 2008;[PubMed]
22. Dexter DT, author; Carter CJ, author; Wells FR, author; Javoy-Agid F, author; Agid Y, author; Lees A, author; Jenner P, author; Marsden CD, author. Basal lipid peroxidation in

substantia nigra is increased in Parkinson's disease. J Neurochem. 52:381–389. 1989; [PubMed]

23. Dinis-Oliveira RJ, author; Remiao F, author; Carmo H, author; Duarte JA, author; Navarro AS, author; Bastos ML, author; Carvalho F, author. Paraquat exposure as an etiological factor of Parkinson's disease. Neurotoxicology. 27:1110–1122. 2006;[PubMed]
24. Drechsel DA, author; Patel M, author. Role of reactive oxygen species in the neurotoxicity of environmental agents implicated in Parkinson's disease. Free Radic Biol Med. 44:1873–1886. 2008;[PubMed]
25. Elbaz A, author; Tranchant C, author. Epidemiologic studies of environmental exposures in Parkinson's disease. J Neurol Sci. 262:37–44. 2007;[PubMed]
26. Fei Q, author; McCormack AL, author; Di Monte DA, author; Ethell DW, author. Paraquat neurotoxicity is mediated by a Bak-dependent mechanism. J Biol Chem. 283:3357–3364. 2008;[PubMed]
27. Franco R, author; Cidlowski JA, author. Apoptosis and glutathione: Beyond an antioxidant. Cell Death Differ. 16:1303–1314. 2009;[PubMed]
28. Franco R, author; Li S, author; Rodriguez-Rocha H, author; Burns M, author; Panayiotidis MI, author. Molecular mechanisms of pesticide-induced neurotoxicity: Relevance to Parkinson's disease. Chem Biol Interact. 188:289–300. 2010;[PubMed]
29. Gallogly MM, author; Starke DW, author; Leonberg AK, author; Ospina SM, author; Mieyal JJ, author. Kinetic and mechanistic characterization and versatile catalytic properties of mammalian glutaredoxin 2: Implications for intracellular roles. Biochemistry. 47:11144–11157. 2008;[PubMed]
30. Gonzalez-Polo R, author; Niso-Santano M, author; Moran JM, author; Ortiz-Ortiz MA, author; Bravo-San Pedro JM, author; Soler G, author; Fuentes JM, author. Silencing DJ-1 reveals its contribution in paraquat-induced autophagy. J Neurochem. 109:889–898. 2009; [PubMed]
31. Goodman SR, author; Zagon IS, author; Riederer BM, author. Spectrin isoforms in mammalian brain. Brain Res Bull. 18:787–792. 1987;[PubMed]
32. Han BS, author; Noh JS, author; Gwag BJ, author; Oh YJ, author. A distinct death mechanism is induced by 1-methyl-4-phenylpyridinium or by 6-hydroxydopamine in cultured rat cortical neurons: Degradation and dephosphorylation of tau. Neurosci Lett. 341:99–102. 2003;[PubMed]
33. Han K, author; Kim MH, author; Seeburg D, author; Seo J, author; Verpelli C, author; Han S, author; Chung HS, author; Ko J, author; Lee HW, author; Kim K, author; Heo WD, author;

Meyer T, author; Kim H, author; Sala C, author; Choi SY, author; Sheng M, author; Kim E, author. Regulated RalBP1 binding to RalA and PSD-95 controls AMPA receptor endocytosis and LTD. PLoS Biol. 7:e1000187 2009;[PubMed]

34. Hayashi T, author; Funato Y, author; Terabayashi T, author; Morinaka A, author; Sakamoto R, author; Ichise H, author; Fukuda H, author; Yoshida N, author; Miki H, author. Nucleoredoxin negatively regulates Toll-like receptor 4 signaling via recruitment of flightless-I to myeloid differentiation primary response gene (88). J Biol Chem. 285:18586–18593. 2010;[PubMed]
35. Henchcliffe C, author; Beal MF, author. Mitochondrial biology and oxidative stress in Parkinson disease pathogenesis. Nat Clin Pract Neurol. 4:600–009. 2008;[PubMed]
36. Ho YS, author; Xiong Y, author; Ho DS, author; Gao J, author; Chua BH, author; Pai H, author; Mieyal JJ, author. Targeted disruption of the glutaredoxin 1 gene does not sensitize adult mice to tissue injury induced by ischemia/reperfusion and hyperoxia. Free Radic Biol Med. 43:1299–1312. 2007;[PubMed]
37. Horowitz MP, author; Greenamyre JT, author. Gene-environment interactions in Parkinson's disease: The importance of animal modeling. Clin Pharmacol Ther. 88:467–474. 2010;[PubMed]
38. Humphries KM, author; Juliano C, author; Taylor SS, author. Regulation of cAMP-dependent protein kinase activity by glutathionylation. J Biol Chem. 277:43505–43511. 2002;[PubMed]
39. Hurd TR, author; Costa NJ, author; Dahm CC, author; Beer SM, author; Brown SE, author; Filipovska A, author; Murphy MP, author. Glutathionylation of mitochondrial proteins. Antioxid Redox Signal. 7:999–1010. 2005;[PubMed]
40. Ikeda M, author; Ishida O, author; Hinoi T, author; Kishida S, author; Kikuchi A, author. Identification and characterization of a novel protein interacting with Ral-binding protein 1, a putative effector protein of Ral. J Biol Chem. 273:814–821. 1998;[PubMed]
41. Janicke RU, author; Ng P, author; Sprengart ML, author; Porter AG, author. Caspase-3 is required for alpha-fodrin cleavage but dispensable for cleavage of other death substrates in apoptosis. J Biol Chem. 273:15540–15545. 1998;[PubMed]
42. Jenner P, author. Altered mitochondrial function, iron metabolism and glutathione levels in Parkinson's disease. Acta Neurol Scand Suppl. 146:6–13. 1993;[PubMed]
43. Johansson M, author; Lundberg M, author. Glutathionylation of beta-actin via a cysteinyl sulfenic acid intermediary. BMC Biochem. 8:26 2007;[PubMed]
44. Kang MJ, author; Gil SJ, author; Koh HC, author. Paraquat induces alternation of the dopamine catabolic pathways and glutathione levels in the substantia nigra of mice. Toxicol

Lett. 188:148–152. 2009;[PubMed]

45. Karunakaran S, author; Saeed U, author; Ramakrishnan S, author; Koumar RC, author; Ravindranath V, author. Constitutive expression and functional characterization of mitochondrial glutaredoxin (Grx2) in mouse and human brain. Brain Res. 1185:8–17. 2007; [PubMed]
46. Kenchappa RS, author; Ravindranath V, author. Glutaredoxin is essential for maintenance of brain mitochondrial complex I: Studies with MPTP. FASEB J. 17:717–719. 2003;[PubMed]
47. Kil IS, author; Park JW, author. Regulation of mitochondrial NADP+-dependent isocitrate dehydrogenase activity by glutathionylation. J Biol Chem. 280:10846–10854. 2005; [PubMed]
48. Lee DW, author; Kaur D, author; Chinta SJ, author; Rajagopalan S, author; Andersen JK, author. A disruption in iron-sulfur center biogenesis via inhibition of mitochondrial dithiol glutaredoxin 2 may contribute to mitochondrial and cellular iron dysregulation in mammalian glutathione-depleted dopaminergic cells: Implications for Parkinson's disease. Antioxid Redox Signal. 11:2083–2094. 2009;[PubMed]
49. Lein ES, author; Hawrylycz MJ, author; Ao N, author; Ayres M, author; Bensinger A, author; Bernard A, author; Boe AF, author; Boguski MS, author; Brockway KS, author; Byrnes EJ, author; Chen L, author; Chen TM, author; Chin MC, author; Chong J, author; Crook BE, author; Czaplinska A, author; Dang CN, author; Datta S, author; Dee NR, author; Desaki AL, author; Desta T, author; Diep E, author; Dolbeare TA, author; Donelan MJ, author; Dong HW, author; Dougherty JG, author; Duncan BJ, author; Ebbert AJ, author; Eichele G, author; Estin LK, author; Faber C, author; Facer BA, author; Fields R, author; Fischer SR, author; Fliss TP, author; Frensley C, author; Gates SN, author; Glattfelder KJ, author; Halverson KR, author; Hart MR, author; Hohmann JG, author; Howell MP, author; Jeung DP, author; Johnson RA, author; Karr PT, author; Kawal R, author; Kidney JM, author; Knapik RH, author; Kuan CL, author; Lake JH, author; Laramee AR, author; Larsen KD, author; Lau C, author; Lemon TA, author; Liang AJ, author; Liu Y, author; Luong LT, author; Michaels J, author; Morgan JJ, author; Morgan RJ, author; Mortrud MT, author; Mosqueda NF, author; Ng LL, author; Ng R, author; Orta GJ, author; Overly CC, author; Pak TH, author; Parry SE, author; Pathak SD, author; Pearson OC, author; Puchalski RB, author; Riley ZL, author; Rockett HR, author; Rowland SA, author; Royall JJ, author; Ruiz MJ, author; Sarno NR, author; Schaffnit K, author; Shapovalova NV, author; Sivisay T, author; Slaughterbeck CR, author; Smith SC, author; Smith KA, author; Smith BI, author; Sodt AJ, author; Stewart NN, author; Stumpf KR, author; Sunkin SM, author; Sutram M, author; Tam A, author; Teemer CD, author; Thaller C, author; Thompson CL, author; Varnam LR, author; Visel A, author;

Whitlock RM, author; Wohnoutka PE, author; Wolkey CK, author; Wong VY, author; Wood M, author; Yaylaoglu MB, author; Young RC, author; Youngstrom BL, author; Yuan XF, author; Zhang B, author; Zwingman TA, author; Jones AR, author. Genome-wide atlas of gene expression in the adult mouse brain. Nature. 445:168–176. 2007;[PubMed]

50. Levy OA, author; Malagelada C, author; Greene LA, author. Cell death pathways in Parkinson's disease: Proximal triggers, distal effectors, and final steps. Apoptosis. 14:478–500. 2009;[PubMed]
51. Li J, author; Yin HL, author; Yuan J, author. Flightless-I regulates proinflammatory caspases by selectively modulating intracellular localization and caspase activity. J Cell Biol. 181:321–333. 2008;[PubMed]
52. Lind C, author; Gerdes R, author; Hamnell Y, author; Schuppe-Koistinen I, author; von Lowenhielm HB, author; Holmgren A, author; Cotgreave IA, author. Identification of S-glutathionylated cellular proteins during oxidative stress and constitutive metabolism by affinity purification and proteomic analysis. Arch Biochem Biophys. 406:229–240. 2002;[PubMed]
53. Lotharius J, author; Dugan LL, author; O'Malley KL, author. Distinct mechanisms underlie neurotoxin-mediated cell death in cultured dopaminergic neurons. J Neurosci. 19:1284–1293. 1999;[PubMed]
54. Mieyal JJ, author; Chock PB, author. Posttranslational modification of cysteine in redox signaling and oxidative stress: Focus on s-glutathionylation. Antioxid Redox Signal. 16:471–475. 2012;[PubMed]
55. Mieyal JJ, author; Gallogly MM, author; Qanungo S, author; Sabens EA, author; Shelton MD, author. Molecular mechanisms and clinical implications of reversible protein S-glutathionylation. Antioxid Redox Signal. 10:1941–1988. 2008;[PubMed]
56. Naoi M, author; Maruyama W, author; Yi H, author; Yamaoka Y, author; Shamoto-Nagai M, author; Akao Y, author; Gerlach M, author; Tanaka M, author; Riederer P, author. Neuromelanin selectively induces apoptosis in dopaminergic SH-SY5Y cells by deglutathionylation in mitochondria: Involvement of the protein and melanin component. J Neurochem. 105:2489–2500. 2008;[PubMed]
57. Nath R, author; Raser KJ, author; Stafford D, author; Hajimohammadreza I, author; Posner A, author; Allen H, author; Talanian RV, author; Yuen P, author; Gilbertsen RB, author; Wang KK, author. Non-erythroid alpha-spectrin breakdown by calpain and interleukin 1 beta-converting-enzyme-like protease(s) in apoptotic cells: Contributory roles of both protease families in neuronal apoptosis. Biochem J. 319:683–690. 1996;[PubMed]

58. Peng J, author; Mao XO, author; Stevenson FF, author; Hsu M, author; Andersen JK, author. The herbicide paraquat induces dopaminergic nigral apoptosis through sustained activation of the JNK pathway. J Biol Chem. 279:32626–32632. 2004;[PubMed]

59. Penninkhof F, author; Grootegoed JA, author; Blok LJ, author. Identification of REPS2 as a putative modulator of NF-kappaB activity in prostate cancer cells. Oncogene. 23:5607–5615. 2004;[PubMed]

60. Perry TL, author; Yong VW, author. Idiopathic Parkinson's disease, progressive supranuclear palsy and glutathione metabolism in the substantia nigra of patients. Neurosci Lett. 67:269–274. 1986;[PubMed]

61. Poole LB, author; Nelson KJ, author. Discovering mechanisms of signaling-mediated cysteine oxidation. Curr Opin Chem Biol. 12:18–24. 2008;[PubMed]

62. Przedborski S, author. Pathogenesis of nigral cell death in Parkinson's disease. Parkinsonism Relat Disord. 11(Suppl 1):S3–7. 2005;[PubMed]

63. Qanungo S, author; Starke DW, author; Pai HV, author; Mieyal JJ, author; Nieminen AL, author. Glutathione supplementation potentiates hypoxic apoptosis by S-glutathionylation of p65-NFkappaB. J Biol Chem. 282:18427–18436. 2007;[PubMed]

64. Ramachandiran S, author; Hansen JM, author; Jones DP, author; Richardson JR, author; Miller GW, author. Divergent mechanisms of paraquat, MPP+, and rotenone toxicity: oxidation of thioredoxin and caspase-3 activation. Toxicol Sci. 95:163–171. 2007;[PubMed]

65. Reynolds A, author; Leake D, author; Boese Q, author; Scaringe S, author; Marshall WS, author; Khvorova A, author. Rational siRNA design for RNA interference. Nat Biotechnol. 22:326–330. 2004;[PubMed]

66. Sabens EA, author; Distler AM, author; Mieyal JJ, author. Levodopa deactivates enzymes that regulate thiol-disulfide homeostasis and promotes neuronal cell death: Implications for therapy of Parkinson's disease. Biochemistry. 49:2715–2724. 2010;[PubMed]

67. Sabens Liedhegner EA, author; Steller KM, author; Mieyal JJ, author. Levodopa activates apoptosis signaling kinase 1 (ASK1) and promotes apoptosis in a neuronal model: Implications for the treatment of Parkinson's disease. Chem Res Toxicol. 24:1644–1652. 2011;[PubMed]

68. Saeed U, author; Durgadoss L, author; Valli RK, author; Joshi DC, author; Joshi PG, author; Ravindranath V, author. Knockdown of cytosolic glutaredoxin 1 leads to loss of mitochondrial membrane potential: Implication in neurodegenerative diseases. PLoS One. 3:e2459 2008;[PubMed]

69. Saeed U, author; Ray A, author; Valli RK, author; Kumar AM, author; Ravindranath V,

author. DJ-1 loss by glutaredoxin but not glutathione depletion triggers Daxx translocation and cell death. Antioxid Redox Signal. 13:127–144. 2010;[PubMed]

70. Schapira AH, author. Mitochondria in the aetiology and pathogenesis of Parkinson's disease. Lancet Neurol. 7:97–109. 2008;[PubMed]
71. Schapira AH, author. Neurobiology and treatment of Parkinson's disease. Trends Pharmacol Sci. 30:41–47. 2009;[PubMed]
72. Shelton MD, author; Kern TS, author; Mieyal JJ, author. Glutaredoxin regulates nuclear factor kappa-B and intercellular adhesion molecule in Muller cells: Model of diabetic retinopathy. J Biol Chem. 282:12467–12474. 2007;[PubMed]
73. Sherer TB, author; Greenamyre JT, author. Oxidative damage in Parkinson's disease. Antioxid Redox Signal. 7:627–629. 2005;[PubMed]
74. Sherer TB, author; Richardson JR, author; Testa CM, author; Seo BB, author; Panov AV, author; Yagi T, author; Matsuno-Yagi A, author; Miller GW, author; Greenamyre JT, author. Mechanism of toxicity of pesticides acting at complex I: Relevance to environmental etiologies of Parkinson's disease. J Neurochem. 100:1469–1479. 2007;[PubMed]
75. Silacci P, author; Mazzolai L, author; Gauci C, author; Stergiopulos N, author; Yin HL, author; Hayoz D, author. Gelsolin superfamily proteins: Key regulators of cellular functions. Cell Mol Life Sci. 61:2614–2623. 2004;[PubMed]
76. Singhal SS, author; Yadav S, author; Drake K, author; Singhal J, author; Awasthi S, author. Hsf-1 and POB1 induce drug sensitivity and apoptosis by inhibiting Ralbp1. J Biol Chem. 283:19714–19729. 2008;[PubMed]
77. Song JJ, author; Rhee JG, author; Suntharalingam M, author; Walsh SA, author; Spitz DR, author; Lee YJ, author. Role of glutaredoxin in metabolic oxidative stress. Glutaredoxin as a sensor of oxidative stress mediated by H2O2. J Biol Chem. 277:46566–46575. 2002; [PubMed]
78. Starke DW, author; Chock PB, author; Mieyal JJ, author. Glutathione-thiyl radical scavenging and transferase properties of human glutaredoxin (thioltransferase). Potential role in redox signal transduction. J Biol Chem. 278:14607–14613. 2003;[PubMed]
79. Sullivan DM, author; Wehr NB, author; Fergusson MM, author; Levine RL, author; Finkel T, author. Identification of oxidant-sensitive proteins: TNF-alpha induces protein glutathiolation. Biochemistry. 39:11121–11128. 2000;[PubMed]
80. Tanner CM, author; Kamel F, author; Ross GW, author; Hoppin JA, author; Goldman SM, author; Korell M, author; Marras C, author; Bhudhikanok GS, author; Kasten M, author; Chade AR, author; Comyns K, author; Richards MB, author; Meng C, author; Priestley B,

author; Fernandez HH, author; Cambi F, author; Umbach DM, author; Blair A, author; Sandler DP, author; Langston JW, author. Rotenone, paraquat and Parkinson's Disease. Environ Health Perspect. 119:866–872. 2011;[PubMed]

81. Tawa P, author; Hell K, author; Giroux A, author; Grimm E, author; Han Y, author; Nicholson DW, author; Xanthoudakis S, author. Catalytic activity of caspase-3 is required for its degradation: Stabilization of the active complex by synthetic inhibitors. Cell Death Differ. 11:439–447. 2004;[PubMed]
82. Tieu K, author. A guide to neurotoxic animal models of Parkinson's disease. Cold Spring Harb Perspect Med. 1:a009316 2011;[PubMed]
83. Tomassi L, author; Costantini A, author; Corallino S, author; Santonico E, author; Carducci M, author; Cesareni G, author; Castagnoli L, author. The central proline rich region of POB1/REPS2 plays a regulatory role in epidermal growth factor receptor endocytosis by binding to 14-3-3 and SH3 domain-containing proteins. BMC Biochem. 9:21 2008;[PubMed]
84. Vance JM, author; Ali S, author; Bradley WG, author; Singer C, author; Di Monte DA, author. Gene-environment interactions in Parkinson's disease and other forms of parkinsonism. Neurotoxicology. 31:598–602. 2010;[PubMed]
85. Wang J, author; Boja ES, author; Tan W, author; Tekle E, author; Fales HM, author; English S, author; Mieyal JJ, author; Chock PB, author. Reversible glutathionylation regulates actin polymerization in A431 cells. J Biol Chem. 276:47763–47766. 2001;[PubMed]
86. Wang J, author; Tekle E, author; Oubrahim H, author; Mieyal JJ, author; Stadtman ER, author; Chock PB, author. Stable and controllable RNA interference: Investigating the physiological function of glutathionylated actin. Proc Natl Acad Sci USA. 100:5103–5106. 2003;[PubMed]
87. Wang KK, author; Posmantur R, author; Nath R, author; McGinnis K, author; Whitton M, author; Talanian RV, author; Glantz SB, author; Morrow JS, author. Simultaneous degradation of alphaII- and betaII-spectrin by caspase 3 (CPP32) in apoptotic cells. J Biol Chem. 273:22490–22497. 1998;[PubMed]
88. Winterbourn CC, author; Hampton MB, author. Thiol chemistry and specificity in redox signaling. Free Radic Biol Med. 45:549–561. 2008;[PubMed]
89. Xing K, author; Lou MF, author. The possible physiological function of thioltransferase in cells. FASEB J. 17:2088–2090. 2003;[PubMed]
90. Xu J, author; Liao L, author; Qin J, author; Liu D, author; Songyang Z, author. Identification of Flightless-I as a substrate of the cytokine-independent survival kinase CISK. J Biol Chem. 284:14377–14385. 2009;[PubMed]

91. Yadav S, author; Zajac E, author; Singhal SS, author; Singhal J, author; Drake K, author; Awasthi YC, author; Awasthi S, author. POB1 over-expression inhibits RLIP76-mediated transport of glutathione-conjugates, drugs and promotes apoptosis. Biochem Biophys Res Commun. 328:1003–1009. 2005;[PubMed]
92. Yao Z, author; Wood NW, author. Cell death pathways in Parkinson's disease: Role of mitochondria. Antioxid Redox Signal. 11:2135–2149. 2009;[PubMed]

[Back]

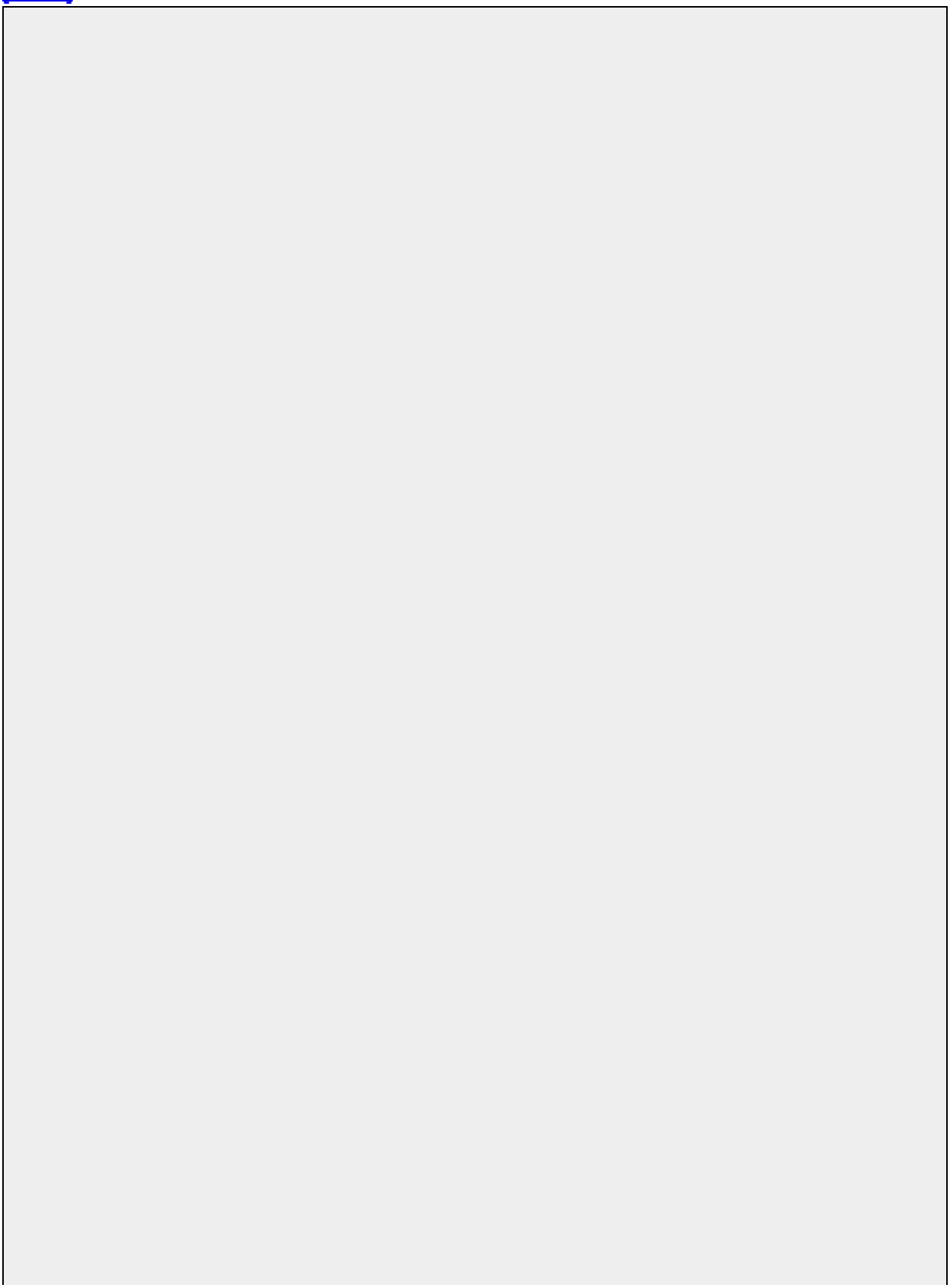

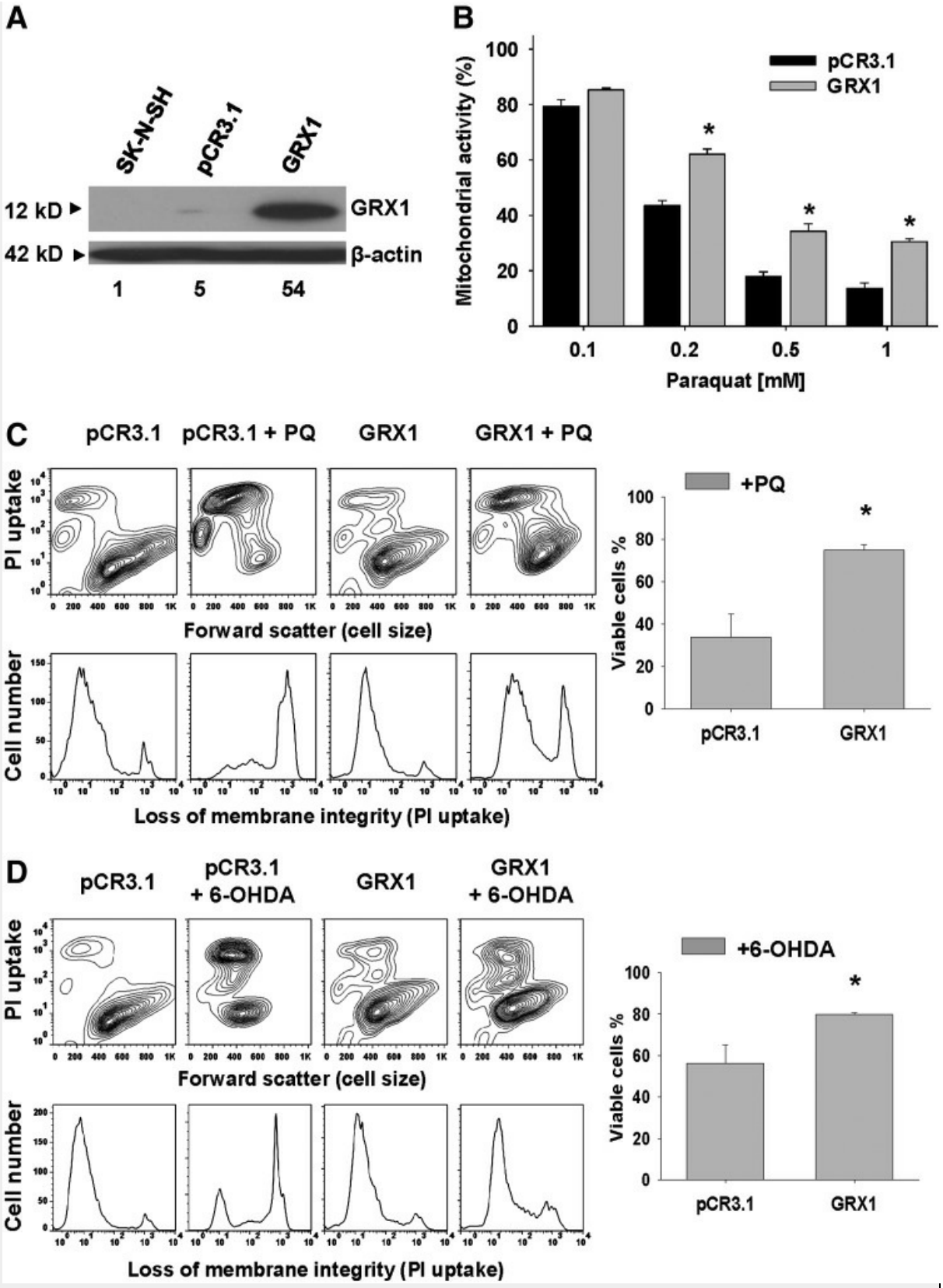
A
SK-N-SH
pCR3.1
GRX1
12 kD
GRX1
42 kD
β-actin
1
5
54
B
Mitochondrial activity (%)
pCR3.1
GRX1
Paraquat [mM]
C
pCR3.1
pCR3.1 + PQ
GRX1
GRX1 + PQ
PI uptake
Forward scatter (cell size)
Cell number
Loss of membrane integrity (PI uptake)
+PQ
Viable cells %
pCR3.1
GRX1
D
pCR3.1
pCR3.1 + 6-OHDA
GRX1
GRX1 + 6-OHDA
PI uptake
Forward scatter (cell size)
Cell number
Loss of membrane integrity (PI uptake)
+6-OHDA
Viable cells %
pCR3.1
GRX1

FIG. 1.

Stable overexpression of GRX1 protects against dopaminergic cell death induced by paraquat and 6-OHDA. Human dopaminergic SK-N-SH cells were stably transfected with empty pCR3.1 vector and pCR3.1 vector encoding human GRX1 **(A)**. In **B–D**, the effect of GRX1 overexpression against cell death induced by a 48 h treatment with paraquat (0.5 m*M* in **C**) or 6-OHDA (50 µ*M*) **(D)** was analyzed by determination of mitochondrial activity **(B)** and cell viability **(C** and **D)**. Mitochondrial activity **(B)** was assessed by measuring the conversion of the tetrazolium salt, MTT. Loss of cell viability or plasma membrane integrity is reflected by the increase in the number of cells with increased PI fluorescence (plots and bar graphs in **C** and **D**). Data in bar graphs represent % of viable cells from paraquat (**C)** and 6-OHDA (**D)** treated cells and are means±SEM of four independent experiments. **p*<0.05, significant difference between GRX1 and pCR3.1 values. Contour plots and Western blots are representative of 2–4 independent experiments. Numbers in **A** represent the densitometry analysis with respect to SK-N-SH cells normalized to β-actin.

[Back]

[Back]

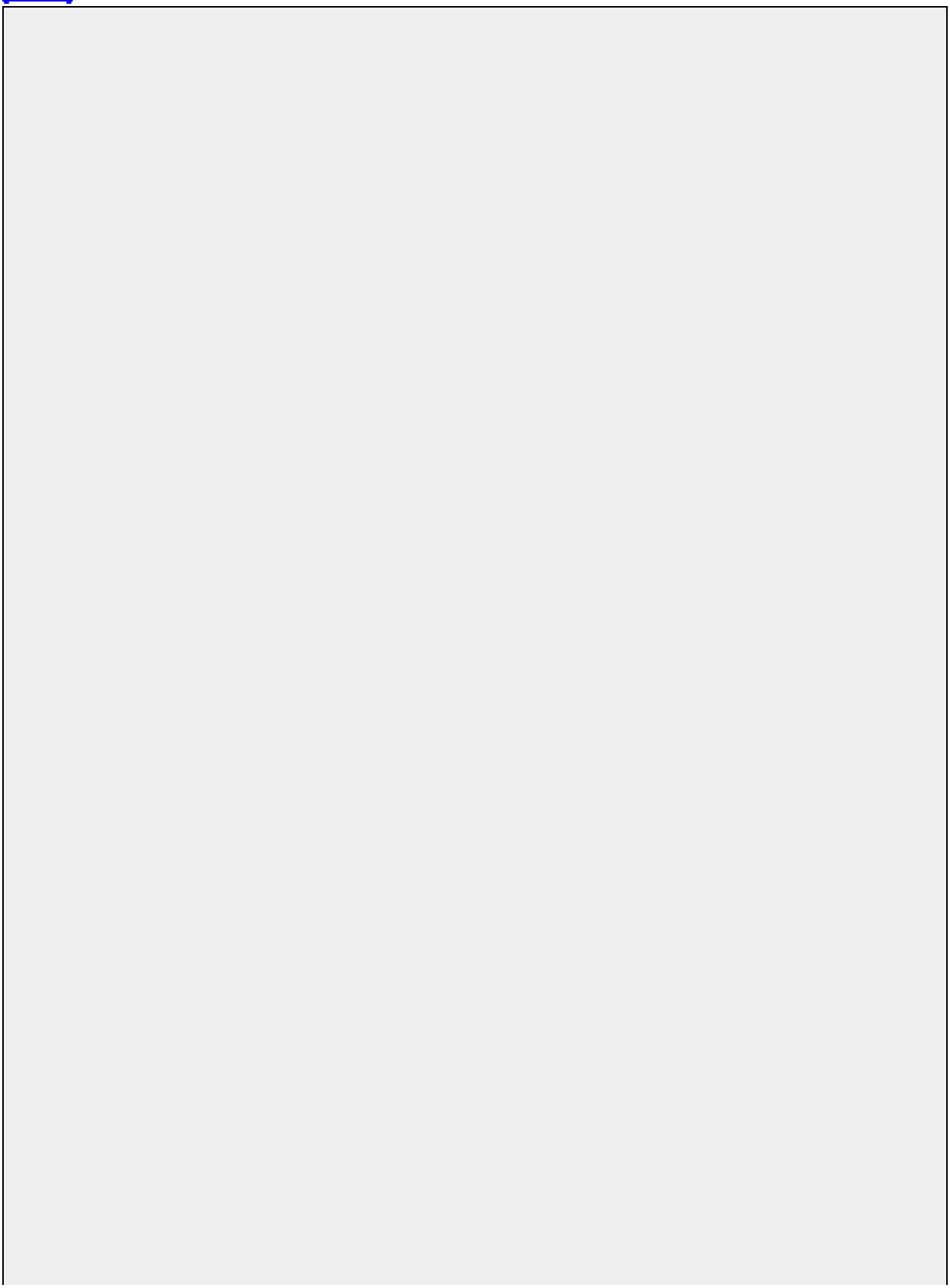

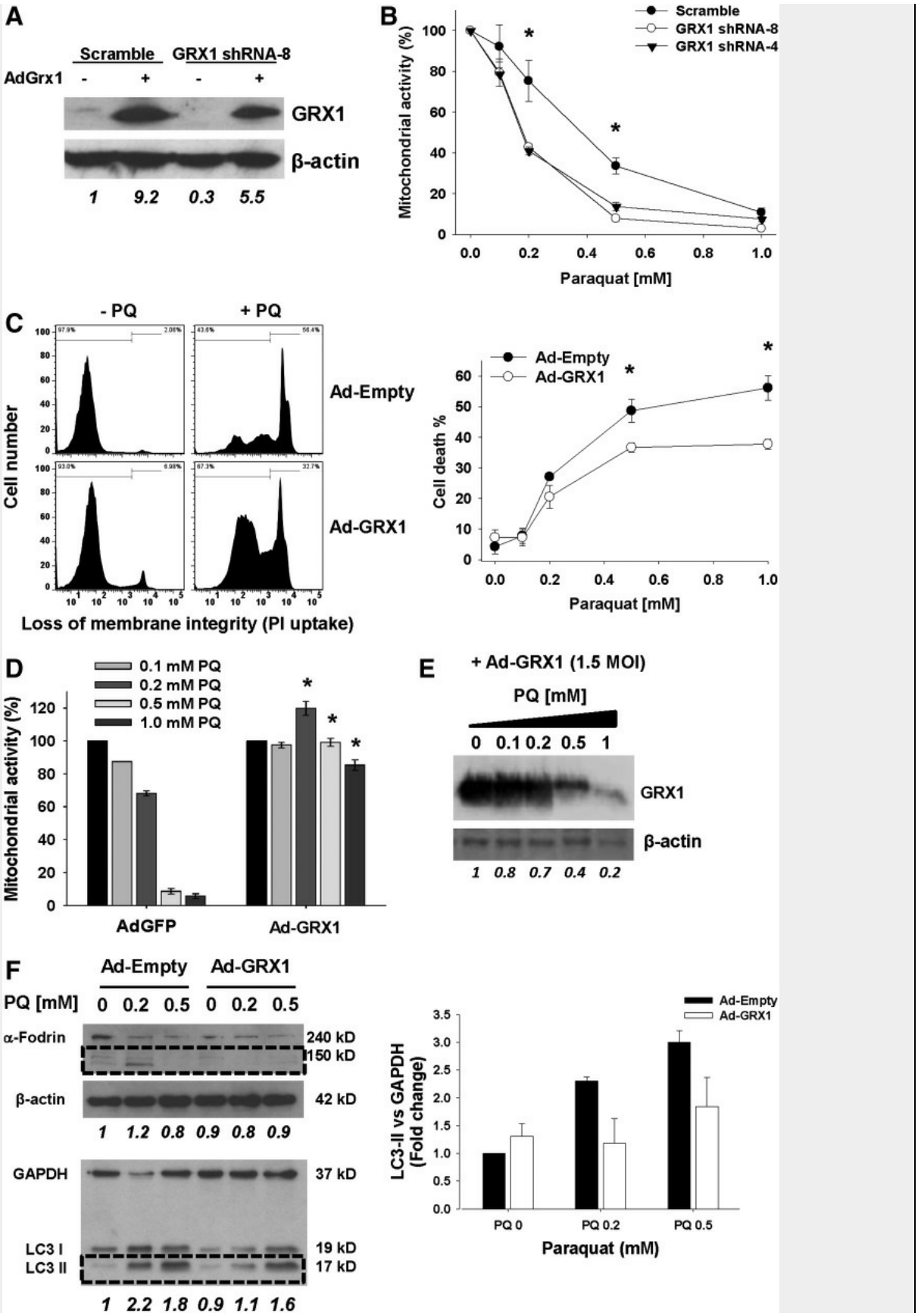
A
Scramble
GRX1 shRNA-8
AdGrx1 - + - +
GRX1
β-actin
1 9.2 0.3 5.5
B
Scramble
GRX1 shRNA-8
GRX1 shRNA-4
Mitochondrial activity (%)
Paraquat [mM]
C
- PQ
+ PQ
Ad-Empty
Ad-GRX1
Cell number
Loss of membrane integrity (PI uptake)
Ad-Empty
Ad-GRX1
Cell death %
Paraquat [mM]
D
0.1 mM PQ
0.2 mM PQ
0.5 mM PQ
1.0 mM PQ
Mitochondrial activity (%)
AdGFP
Ad-GRX1
E
+ Ad-GRX1 (1.5 MOI)
PQ [mM]
0 0.1 0.2 0.5 1
GRX1
β-actin
1 0.8 0.7 0.4 0.2
F
Ad-Empty
Ad-GRX1
PQ [mM] 0 0.2 0.5 0 0.2 0.5
α-Fodrin
240 kD
150 kD
β-actin
42 kD
1 1.2 0.8 0.9 0.8 0.9
GAPDH
37 kD
LC3 I
LC3 II
19 kD
17 kD
1 2.2 1.8 0.9 1.1 1.6
Ad-Empty
Ad-GRX1
LC3-II vs GAPDH (Fold change)
PQ 0
PQ 0.2
PQ 0.5
Paraquat (mM)

FIG. 2.

Adenovirus-mediated overexpression of GRX1 and shRNA knock-down regulate dopaminergic cell death induced by paraquat. Overexpression of GRX1 by recombinant adenovirus Ad5CMV-GRX1 (1.5 MOI) and GRX1 knock-down with shRNA lentiviral particles were determined by Western blot **(A)**. The effect of GRX1 overexpression **(C** and **D)** and knock-down **(B)** on the loss of mitochondrial activity **(B** and **D)** and cell death **(C)** induced by paraquat was determined as in Figure 1. In **E**, the effect of paraquat (48 h treatment) on the overexpression of GRX1 induced by Ad5CMV-GRX1 (1.5 MOI) was evaluated. Cleavage of α-fodrin (apoptotic marker) and accumulation of LC3-II (autophagy marker) induced by paraquat were also determined by Western blot in whole cell lysates **(F)**. Control adenovirus contained only the cytomegalovirus promoter (AdEmpty) and/or the green fluorescent protein gene as a reporter (AdGFP). Data in graphs represent means ±SEM of four independent experiments. **p*<0.05, shRNA4 and 8 vs Scramble **(C)**, or GRX1 *vs.* Empty values **(D)**. Plots in **(C)** represent 0.5 m*M* PQ treatments. Contour plots and Western blots are representative of 3–4 independent experiments. Numbers in blots (*italics*) represent the densitometry analyses with respect to Scramble **(A)**, Ad-GRX1 **(E)**, and Ad-Empty samples **(F)** normalized to β-actin or GAPDH.

[Back]

[Back]

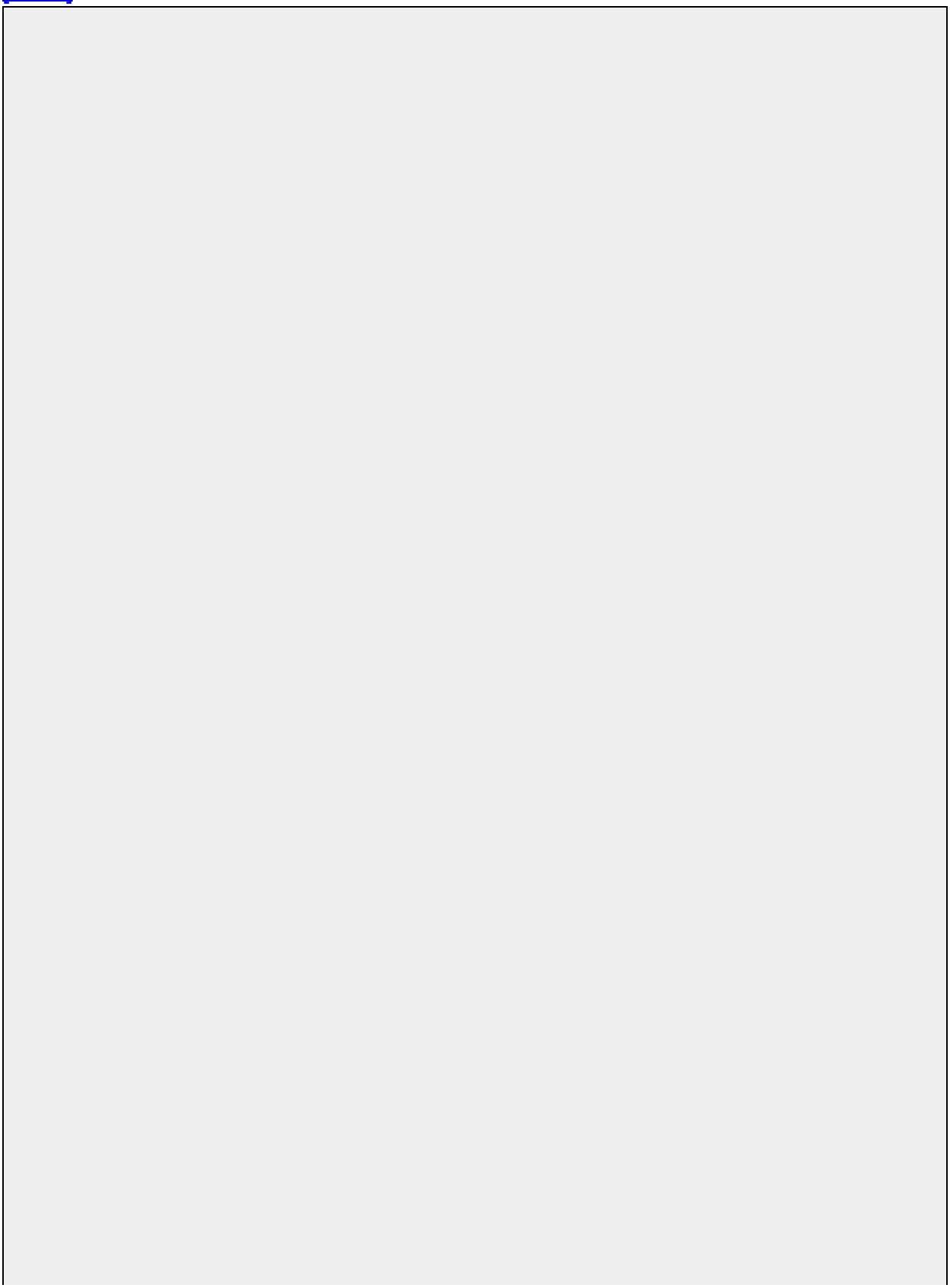

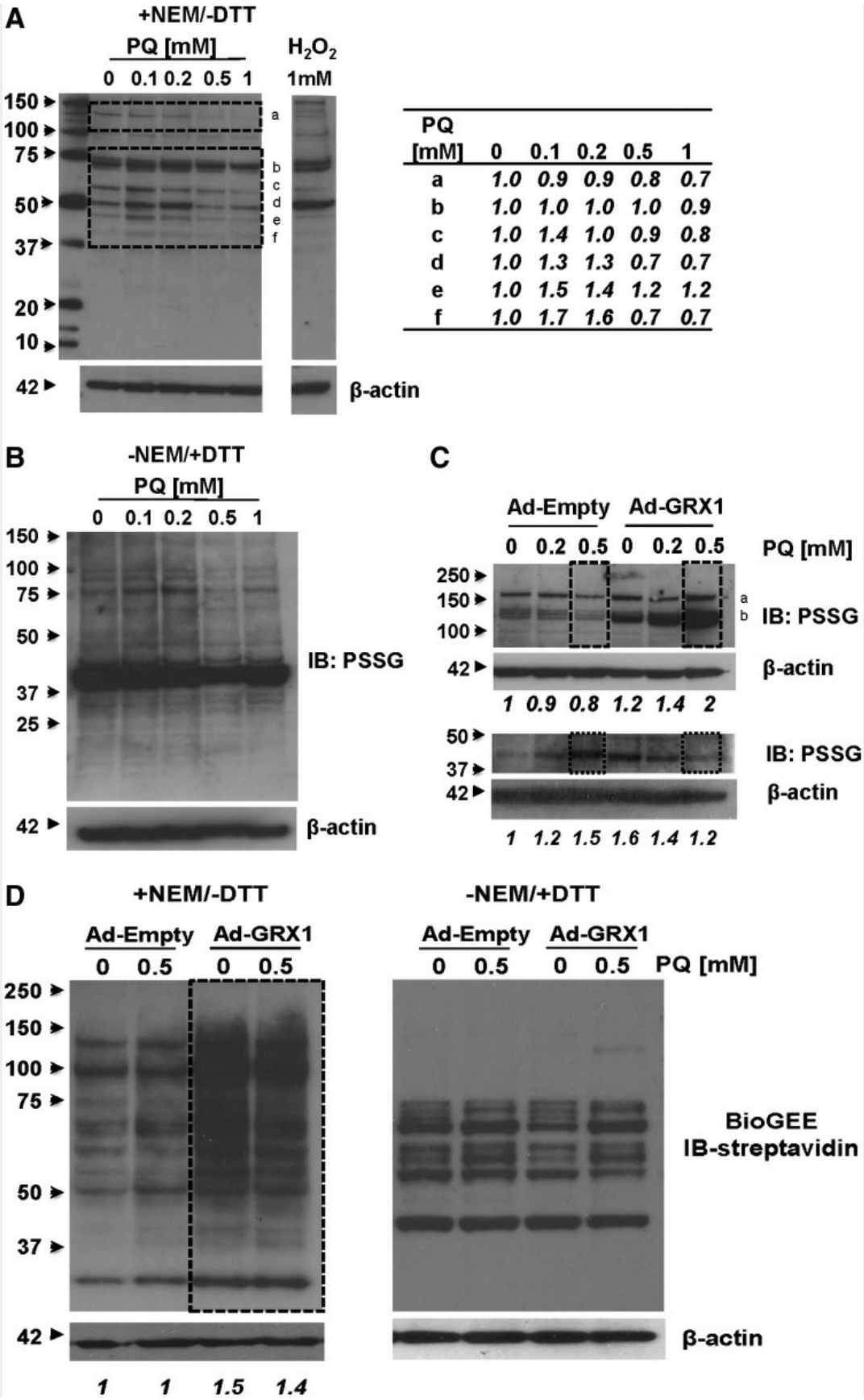
A
+NEM/-DTT
PQ [mM]
0 0.1 0.2 0.5 1
H2O2
1mM
150
100
75
50
37
20
10
42
a
b
c
d
e
f
β-actin
PQ [mM] 0 0.1 0.2 0.5 1
a 1.0 0.9 0.9 0.8 0.7
b 1.0 1.0 1.0 1.0 0.9
c 1.0 1.4 1.0 0.9 0.8
d 1.0 1.3 1.3 0.7 0.7
e 1.0 1.5 1.4 1.2 1.2
f 1.0 1.7 1.6 0.7 0.7
B
-NEM/+DTT
PQ [mM]
0 0.1 0.2 0.5 1
150
100
75
50
37
25
42
IB: PSSG
β-actin
C
Ad-Empty Ad-GRX1
0 0.2 0.5 0 0.2 0.5
PQ [mM]
250
150
100
42
a
b
IB: PSSG
β-actin
1 0.9 0.8 1.2 1.4 2
50
37
42
IB: PSSG
β-actin
1 1.2 1.5 1.6 1.4 1.2
D
+NEM/-DTT
Ad-Empty Ad-GRX1
0 0.5 0 0.5
250
150
100
75
50
37
42
1 1 1.5 1.4
-NEM/+DTT
Ad-Empty Ad-GRX1
0 0.5 0 0.5 PQ [mM]
BioGEE
IB-streptavidin
β-actin

FIG. 3.

Paraquat-induced alterations in glutathionylated proteins. Whole cell lysates of cells treated with or without paraquat for 48 h were isolated and analyzed under reducing (-NEM/+DTT) and nonreducing (+NEM/-DTT) conditions. In **A** and **B**, protein glutathionylation was assessed using anti-PSSG antibody in samples isolated in the presence or absence of >30 m*M* NEM. In **C**, overexpression of GRX1 was induced via adenoviral transduction (1.5 MOI) as described in Figure 2. **C** represents a composite of two independent Western blot with their corresponding loading controls. In **D**, protein glutathionylation was assessed as previously described in cells labeled with BioGEE (250 µ*M*) 1 h prior to experimental treatments, and glutathionylated proteins were visualized using streptavidin-HRP conjugate. Blots were probed with β-actin to determine equal loading. Blots are representative of at least 3 independent experiments. Numbers in blots (*italics*) represent the densitometry analyses with respect to control **(A,** *table***)**, and Ad-Empty samples **(C** and **D)** normalized to β-actin.

[Back]

[Back]

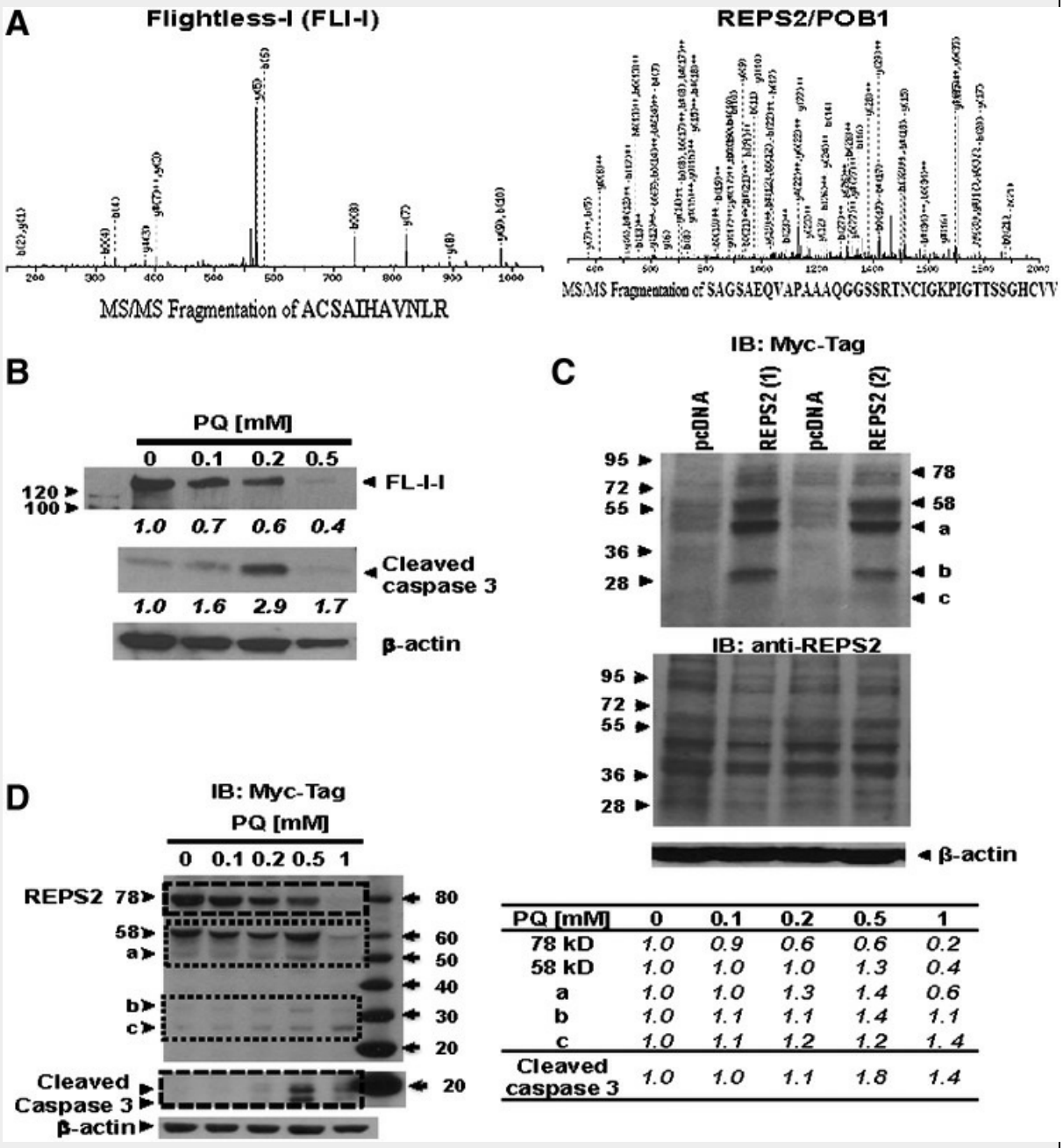

PQ [mM]	0	0.1	0.2	0.5	1
78 kD	1.0	0.9	0.6	0.6	0.2
58 kD	1.0	1.0	1.0	1.3	0.4
a	1.0	1.0	1.3	1.4	0.6
b	1.0	1.1	1.1	1.4	1.1
c	1.0	1.1	1.2	1.2	1. 4
Cleaved caspase 3	1.0	1.0	1.1	1.8	1.4

FIG. 4.

Paraquat toxicity is associated with downregulation of FLI-I and REPS2. (A) Glutathionylated proteins immunoprecipitated with anti-PSSG antibody were processed for mass spectrometry. Samples were digested with trypsin and peptides were subjected to LC/MS/MS analysis using reverse phase chromatography mass spectrometry. Two of the acquired spectrum of peptides identified by mass spectrometry analysis corresponded to FLI-I (ACSAIHAVNLR) and REPS2

SAGSAEQVAPAAAQGGSSRTNCIGKPIGTTSSGHCVV), identified using a human data base (IPI-Human, NCBI). (See Supplementary Fig. S1 for a magnification of the MS spectra). Alterations in the levels of FLI-I, REPS2 and cleaved caspase 3 induced by paraquat were assessed in wild-type **(B)** and stable SK-N-SH overexpressing Myc-His REPS2 **(D)**. In **(C)** and **(D)**, REPS2 protein levels were visualized in stable Myc-His REPS2 overexpressing clones (clone 2 was used in **D**) using anti-myc-tag (*upper panel*) or anti-REPS2 (K-18) (*lower panel*) antibody. a–c labels in **C** and **D** (including the table) represent possible isoforms or degradation products of REPS2. Blots were reprobed with β-actin to corroborate equal loading and are representative of at least 3 independent experiments. Table corresponds to the densitometry analysis of protein bands in **D**. Numbers (*italics*) in **(B)** and **(D)** represent the densitometry analyses with respect to control samples (**D,** *table*) normalized to β-actin.

[Back]

[Back]

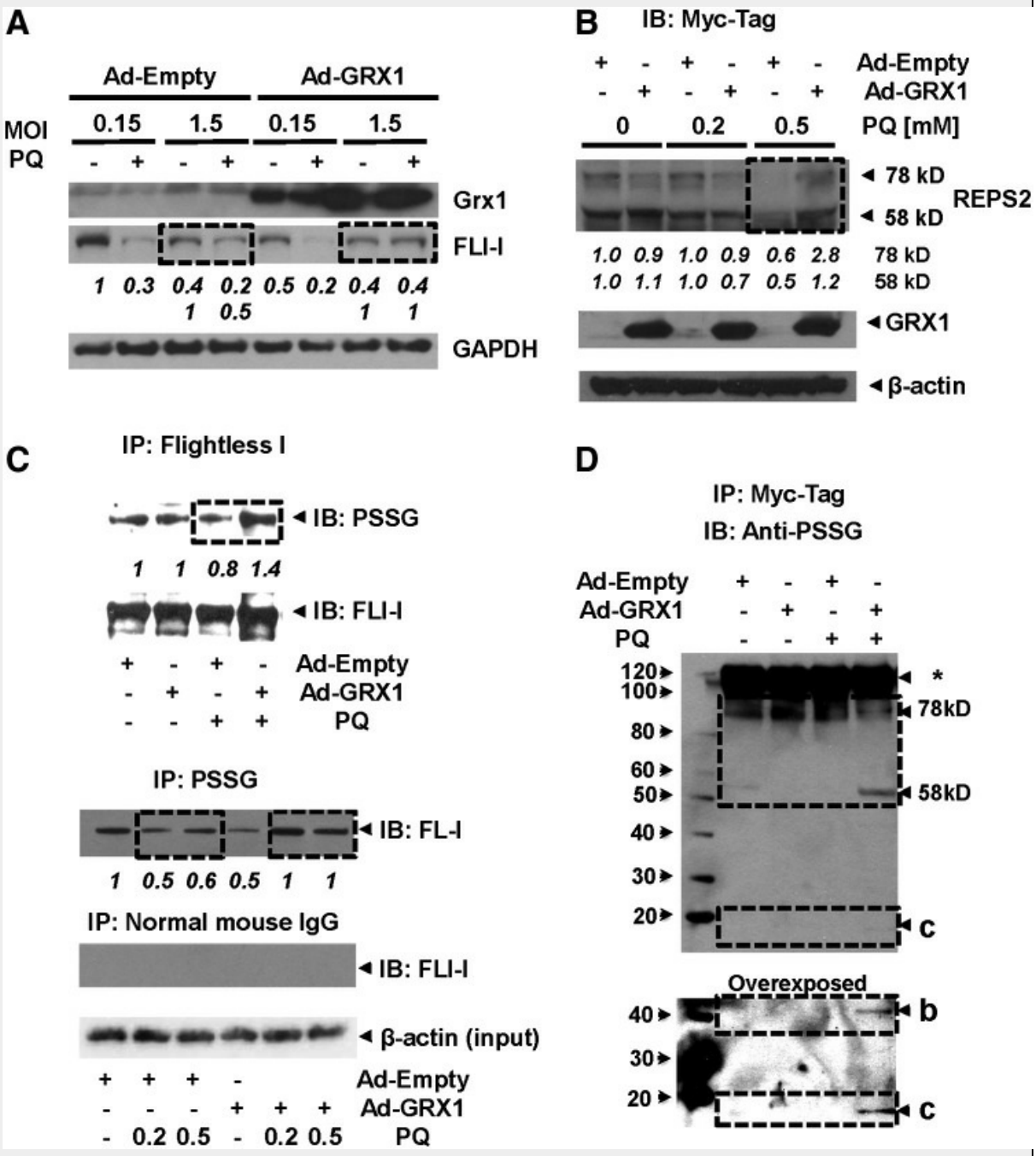

FIG. 5.

GRX1 regulates protein expression levels and glutathionylation of FLI-I and REPS2. In **(A)** and **(B)**, overexpression of GRX1 (Ad-GRX1) reduced paraquat-induced FLI-I and REPS2 downregulation (*broken line rectangles*). SK-N-SH (**A** and **C**) and cells stably expressing Myc/His REPS2 (**B** and **D**) were infected with Ad-

Empty or Ad-GRX1 (1.5 MOI) for 24 h and subsequently treated with paraquat (0.2 m*M* in **A, C** *upper panel*, and **D**) for 48 h. Samples were collected under nonreducing conditions (+NEM/-DTT). In **C** (*upper panel*) and **D**, FLI-I and REPS2 were immunoprecipitated with anti-FLI-I or anti-MycTag antibodies respectively, and then, PSSG were visualized using anti-PSSG antibody. Blot in **(C,** *upper panel***)** was reprobed with anti-FLI-I to corroborate equal levels of immunoprecipitated proteins. In (**C**, *lower panel*), glutathionylated proteins were immunoprecipiated with anti-PSSG antibody and FLI-I levels were visualized using the corresponding antibody. As controls, samples were pre-cleared with Dynabeads coupled with normal mouse IgG. Normal mouse IgG did not pull down FLI-I. Blots are representative of at least 3 independent experiments. Numbers in blots (*italics*) represent the densitometry analyses with respect to Ad-Empty samples [0.15 MOI, upper numbers; and 1.5 MOI lower numbers in **(A)**], normalized to the corresponding loading/input control.

[Back]

[Back]

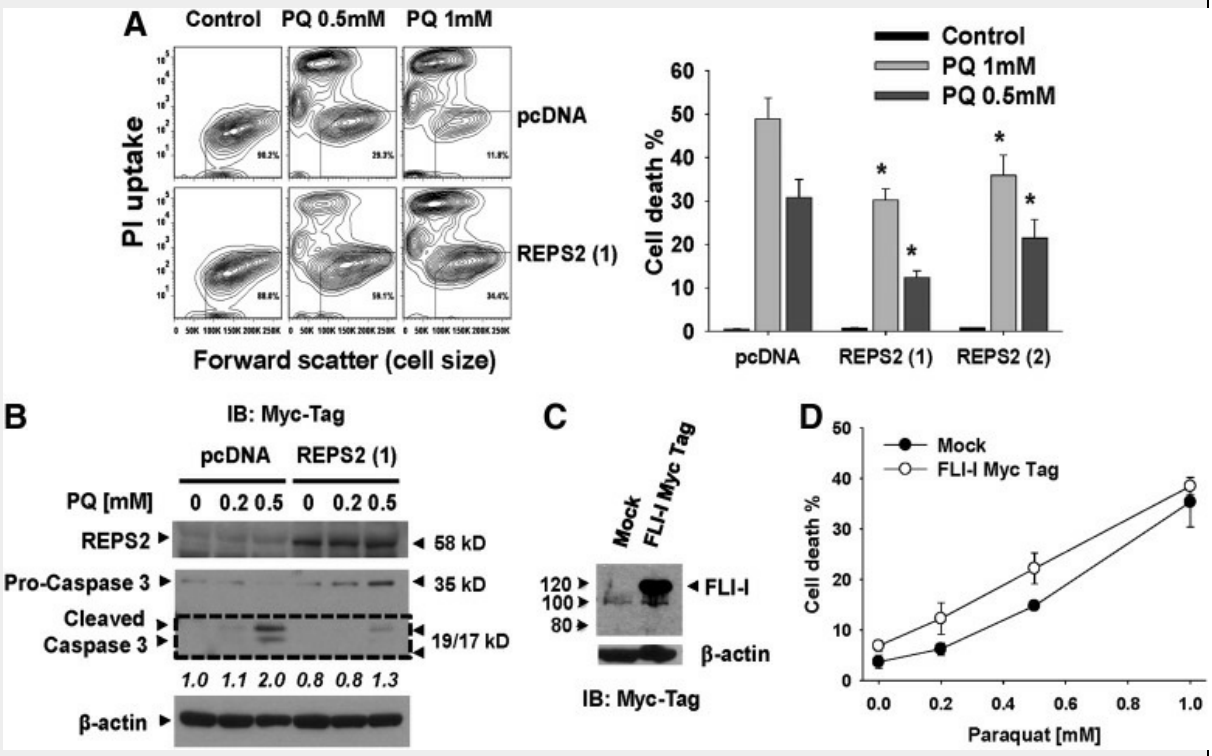

FIG. 6.

Paraquat-induced dopaminergic cell death is significantly reduced by REPS2/POB1 overexpression. (A) SK-N-SH cells overexpressing empty pcDNA3.1 or Myc-His REPS2 were treated with paraquat for 48 h. Cell death was determined by the loss of plasma membrane integrity (PI uptake) and cell shrinkage as a marker of apoptosis. % of dead cells in **A** (*bar graph*) reflects the number of cells with increased PI fluorescence using two distinct clones overexpressing Myc-His REPS2 (See Fig. 4C). In **B**, paraquat-induced cleavage/activation of caspase 3 in both pcDNA3.1 and REPS2 overexpressing cells was evaluated as explained in Figure 2. In **C** and **D**, cells were transiently transfected with Myc-tagged FLI-I for 24 h prior paraquat treatment. Expression levels of FLI-I were corroborated by Western blot **(C)** and the effect of FLI-I overexpression on paraquat-induced dopaminergic cell death was determined as explained in **A**. Data in **A** (*bar graphs*) and **D** are means±SEM of four independent experiments. *$p<0.05$, significant difference between the corresponding REPS2 and pcDNA3.1 values. Contour plots and western blots are representative of 3–4 independent experiments. Numbers in **B** (*italics*) represent the densitometry analyses of cleaved caspase 3 with respect to pcDNA normalized to β-actin.

[Back]

[Back]

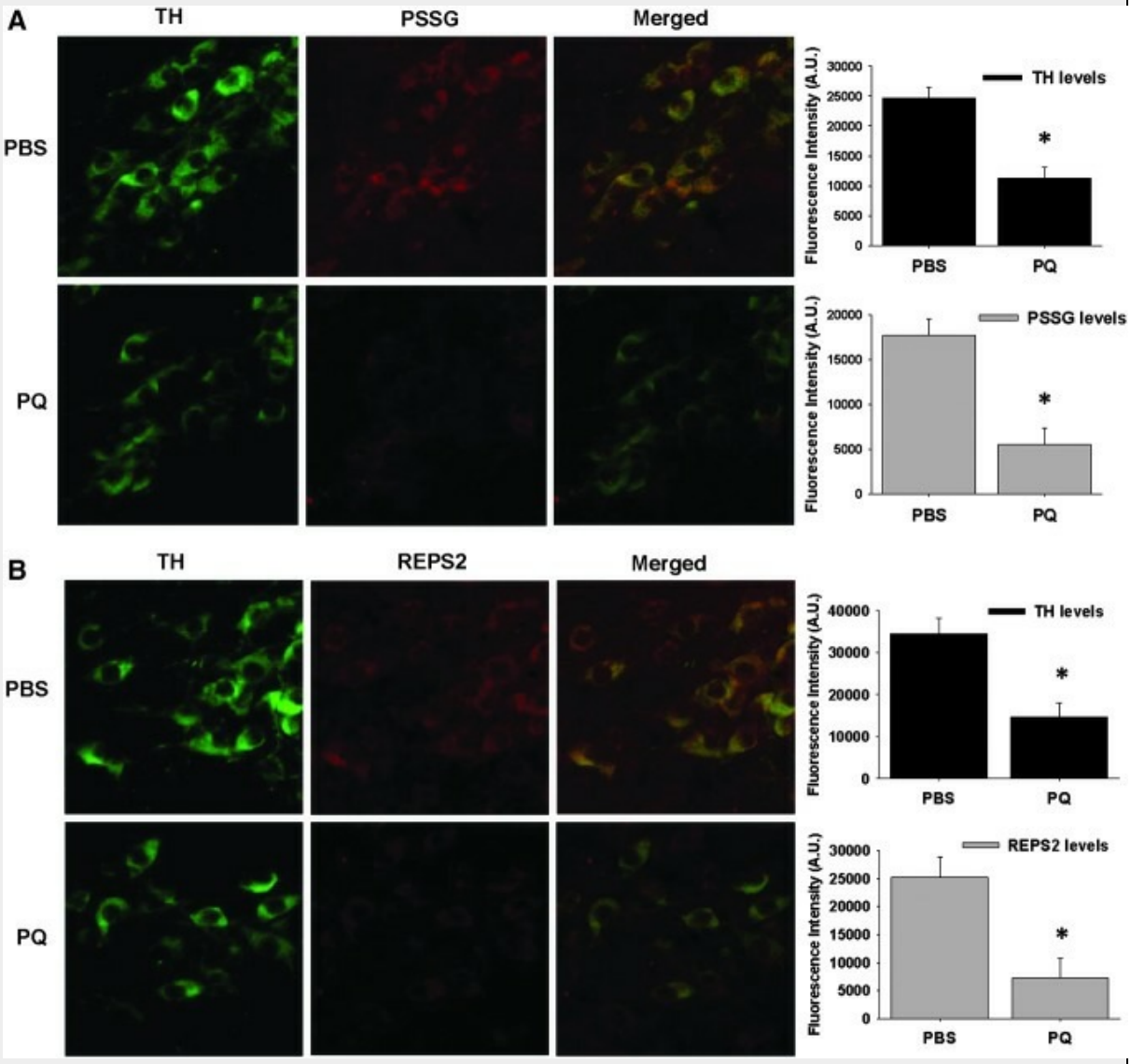

FIG. 7.

Alterations in PSSG and REPS2 in the substantia nigra of mice treated with paraquat. C57BL/6 mice (8–10 weeks old) were administered two intraperitoneal injections of 10 mg/kg PQ or PBS every week for 3 consecutive weeks. Animals were analyzed 1 week after the last injection and coronal sections of the substantia nigra were stained with anti-TH **(A** and **B)** and anti-PSSG **(A)** or anti-REPS2 **(B)** antibody. Sections were incubated in secondary Alexa 488-anti-rabbit (TH) and Alexa 633-anti-mouse (PSSG and REPS2). Sections were mounted with VectaShield and images were collected on a LSM 5 Exciter confocal scanning fluorescent microscope (20 ×) and Zen 2008 software (Carl Zeiss). Fluorescence intensity analysis was performed using ImageJ (NIH) software. Corrected total cell

fluorescence (CTCF) was obtained and expressed as Arbitrary Fluorescence Intensity Units (A.U.).

[Back]

[Back]

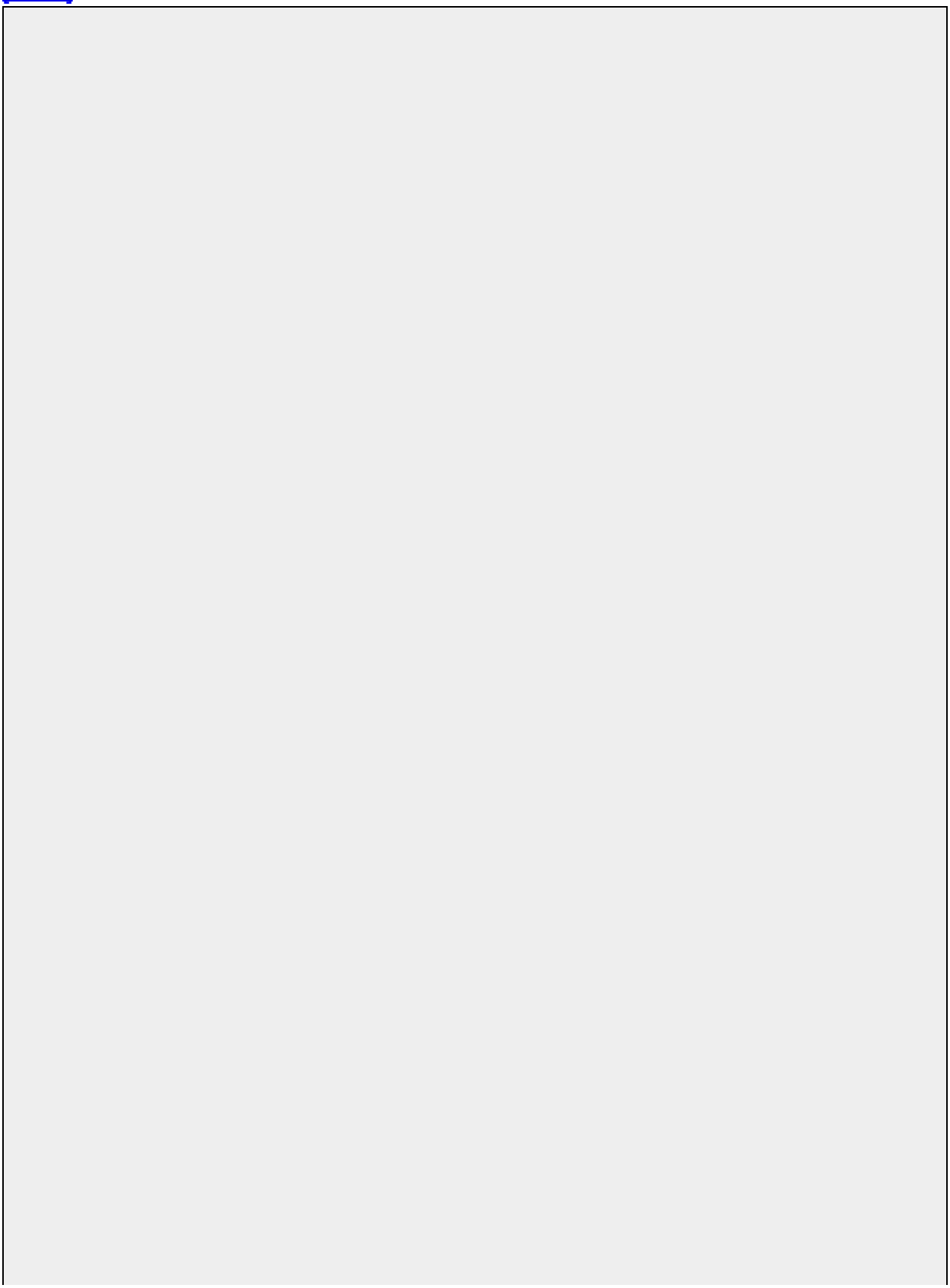

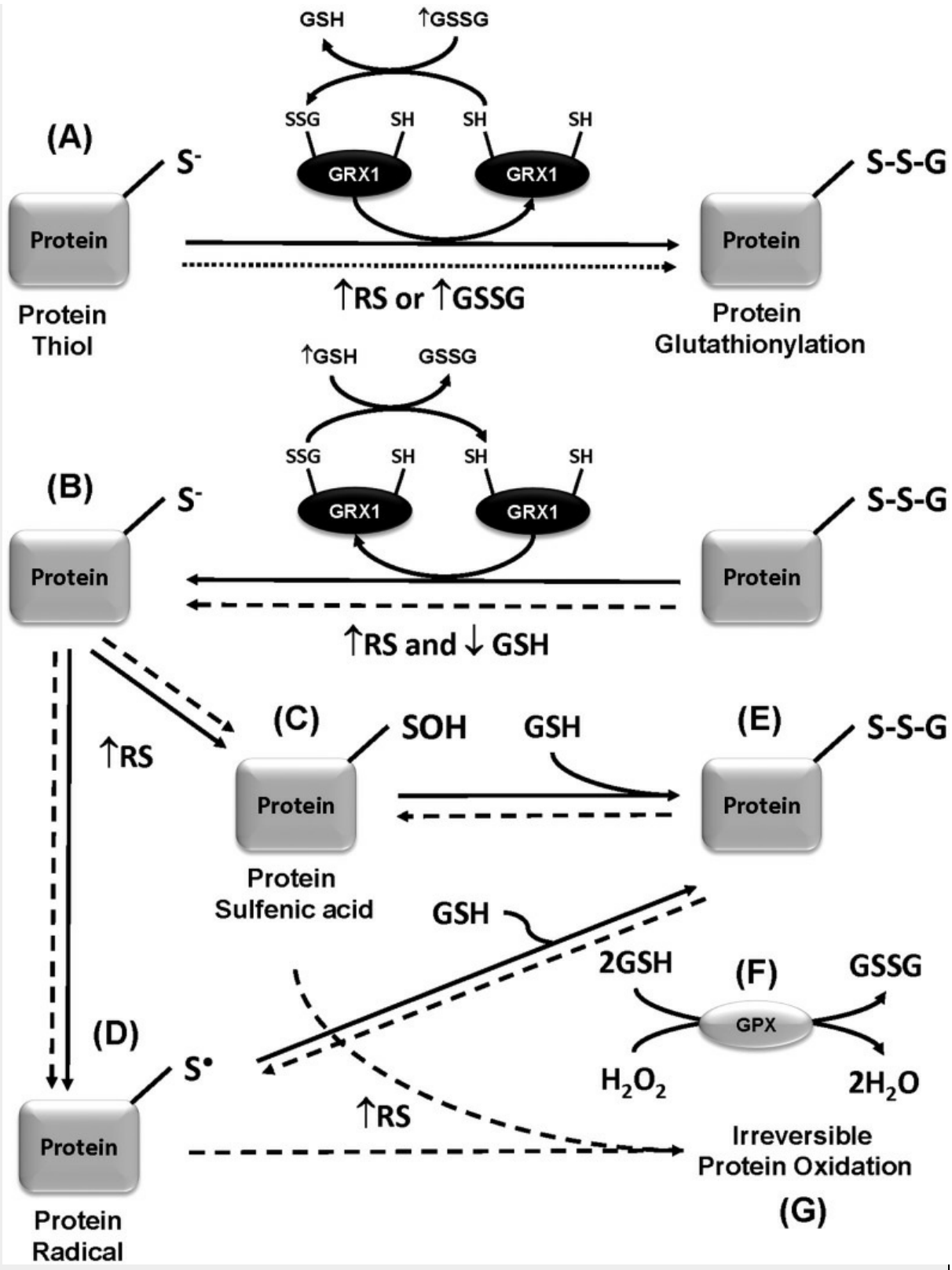
GSH
↑GSSG
SSG
SH
SH
SH
(A)
S-
GRX1
GRX1
S-S-G
Protein
Protein
Protein
Thiol
↑RS or ↑GSSG
Protein
Glutathionylation
↑GSH
GSSG
SSG
SH
SH
SH
(B)
S-
GRX1
GRX1
S-S-G
Protein
Protein
↑RS and ↓ GSH
↑RS
(C)
SOH
GSH
(E)
S-S-G
Protein
Protein
Protein
Sulfenic acid
GSH
2GSH
(F)
GSSG
(D)
GPX
S•
H_2O_2
$2H_2O$
↑RS
Irreversible
Protein Oxidation
Protein
Radical
(G)

FIG. 8.

Proposed mechanism by which paraquat-induced oxidative stress and GRX1 might regulate protein glutathionylation and deglutathionylation distinctively. Protein glutathionylation has been demonstrated to occur by a variety of mechanisms, reviewed in (55, 88). **(A)** PSSG formation might occur by thiol exchange reactions between protein cysteines and GSSG, but this mechanism requires unusually high redox potential. Interestingly, under oxidizing conditions (low GSH/GSSG ratio) GRX1 can use GSSG to promote PSSG formation. Paraquat-induced↑RS might enhance GRX1-mediated glutathionylation by increasing the GSSG pool (*dotted line*). **(B)** Under reducing conditions, GRX1 utilizes the reducing power of GSH to catalyze protein deglutathionylation. Paraquat-induced reactive species (↑ RS) formation might prevent GRX1-mediated deglutathionylation by depletion of intracellular GSH content (*broken lines*). On the other hand, two (H_2O_2, $\bullet ONOO^-$) or one-electron ($\bullet O_2^-$) cysteine oxidation by RS leads to the formation of reactive intermediates including cysteine sulfenic acids (PSOH) **(C)** and protein thiyl radicals (PS•) **(D)**, respectively, which can participate in disulfide bond formation with GSH leading to PSSG formation **(E)**. In addition, GS• generation by oxidative stress has been shown to lead to PSSG formation catalyzed by GRXs (not depicted here). This is another potential mechanism by which GRX1 overexpression might increase protein glutathionylation upon paraquat exposure. Paraquat-induced RS formation and GSH depletion mediated by increased activation of glutathione peroxidase (GPX) (*broken lines)* might enhance cysteine oxidation and also prevent/reverse cysteine glutathionylation leading to their irreversible oxidation **(G)**. Thus, glutathionylation/deglutathionylation depends on the spacial localization of the targeted protein, surrounding redox environment, the nature of the RS involved and expression levels of GRXs **(F)**.

[Back]

Table of Contents